European Journal of Medicinal Chemistry 46 (2011) 5293–5309

Contents lists available at SciVerse ScienceDirect

European Journal of Medicinal Chemistry

journal homepage: http://www.elsevier.com/locate/ejmech

Original article

Synthesis and biological evaluation of novel pyrazole derivatives with anticancer activity

Alessandro Balbi[a,*], Maria Anzaldi[a], Chiara Macciò[a], Cinzia Aiello[b], Mauro Mazzei[a], Rosaria Gangemi[b], Patrizio Castagnola[c], Mariangela Miele[a], Camillo Rosano[d], Maurizio Viale[b]

[a] Dipartimento di Scienze Farmaceutiche, Università degli Studi di Genova, V.le Benedetto XV, 3, 16132 Genova, Italy
[b] Istituto Nazionale per la Ricerca sul Cancro, S.C. Terapia Immunologica, L.go R. Benzi 10, 16132 Genova, Italy
[c] Istituto Nazionale per la Ricerca sul Cancro, S.S. Biofisica e Citometria, L.go R. Benzi 10, 16132 Genova, Italy
[d] Istituto Nazionale per la Ricerca sul Cancro, S.C. Nanobiotecnologie, L.go R. Benzi 10, 16132 Genova, Italy

ARTICLE INFO

Article history:
Received 20 April 2011
Received in revised form
19 July 2011
Accepted 9 August 2011
Available online 31 August 2011

Keywords:
Pyrazole derivatives
Antitumor activity
Apoptosis
Tubulin polymerization inhibitors

ABSTRACT

We synthesized thirty-six novel pyrazole derivatives and studied their antiproliferative activity in human ovarian adenocarcinoma A2780 cells, human lung carcinoma A549 cells, and murine P388 leukemia cells.

Four of these substances were selected because of their higher antiproliferative activity and further analyses showed that they were all able to induce apoptosis, although to a different extent. The expression of p53 and $p21^{waf1}$, which induce apoptosis and cell cycle arrest, was evaluated by western blot analysis in cells treated with compound **12d**.

The analysis of the cell cycle showed that all the selected compounds cause a partial G2/M block and the formation of polyploid cells. Furthermore, the four selected compounds were tested for their interaction with the microtubular cytoskeletal system by docking analysis, tubulin polymerization assay and immunofluorescence staining, demonstrating that the compound **12d**, unlike the other active derivatives, was able to significantly bind dimers of α- and β-tubulin, probably causing a molecular distortion resulting in the disassembly of microtubules.

1. Introduction

The pyrazole scaffold represents a common motif in many pharmaceutical active and remarkable compounds demonstrating a wide range of pharmacological activities; the most important activities are the anti-inflammatory [1,2], the antibacterial-antifungal [3,4], the hypoglycemic [5,6], the anti-hyperlipidemic [7], the inhibition of cyclooxigenase-2 [8], p38 MAP kinase [9] and CDK2/Cyclin A [10,11], and the antiangiogenic [12]. Heterocyclic rings and, in particular, the pyrazole ring, represent an advantageous choice for the synthesis of pharmaceutical compounds with different activities and good safety profiles [13]. Different pyrazole derivatives have also been tested for their antiproliferative activities in vitro and antitumor activity in vivo, often resulting in promising lead compounds [14–18].

Our research started some time ago with the synthesis of heterocyclic ionone-like derivatives, which have a similarity to the so-called 'short heteroretinoids'. These compounds, formed by a cyclohexenyl group linked to a heterocyclic moiety by a short ethenylic chain, have shown antimicrobial [19], anti-inflammatory and histoprotective properties [20]. The heterocyclic moiety (pyrazole, isoxazole, pyrimidine) and the substituents present in them, deeply affected the biological activities. Our researches demonstrated that these compounds have antiproliferative and pro-apoptotic activities. Our attention was focused on a class of ionone-derived 1,5-pyrazoles **1a-f** that exhibited promising antiproliferative properties in preliminary experiments on the HL-60 leukemia cell line (Chart 1) [21]. In particular **1a**, **1d-f** inhibited HL-60 cell growth and induced apoptosis in dose dependent manner, while **1b-c** displayed antiproliferative activity but were unable to induce apoptosis.

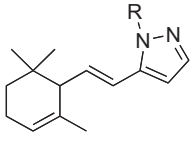

1a-f

1a: R=C(S)N(CH_3)$_2$
1b: R=4-ClC_6H_4
1c: R=4-BrC_6H_4
1d: R=4-(COOEt)C_6H_4
1e: R=3-OH$C_6H_4CH_2$
1f: R=2-pyridinyl

Chart 1. Chemical structure of previous reported compounds **1**.

* Corresponding author. Tel.: +39 0103533040; fax: +39 0103533009.
E-mail address: balbi@unige.it (A. Balbi).

0223-5234/$ – see front matter © 2011 Elsevier Masson SAS. All rights reserved.
doi:10.1016/j.ejmech.2011.08.014

Prompted by the above-mentioned results, we further optimized this chemical series by exploring additional modifications. Firstly we introduced new substituents in the N position of the pyrazole (compd. **4**) also changing the linker moiety in one example (**4h**). Then, keeping the same pyrazole scaffold that showed the best results on HL-60 cells, we planned to synthesize two new sets of molecules: in the first set we chose to remove the cyclohexenyl ring maintaining the ethenylic chain (A), while in the second set we also removed the ethenylic chain (B). Finally we evaluated the importance of introducing a third substituent in the pyrazole ring (C) (Fig. 1).

All the synthesized compounds were preliminarily evaluated for their antiproliferative activity in A2780 (ovary, adenocarcinoma) and A549 (lung, carcinoma) human cell lines, and in murine P388 (leukemia) cells by MTT assay. **12a**, **12a1**, **12d**, **12d1**, the most active compounds in the preliminary screening, have been further evaluated for their ability to induce apoptosis in all the above-mentioned cell lines. In addition, to verify the involvement of **12d** in apoptotic triggering we analyzed the expression of p53 and $p21^{waf1}$ proteins both involved in the induction of apoptosis and cell cycle arrest. On the basis of the results of these studies, which suggest the involvement of the microtubule cytoskeletal system in the mechanism of the action of **12d**, we performed a docking analysis, using the dimer of α- and β-tubulin as the putative target for our molecules, and a tubulin polymerization assay.

2. Chemistry

Compounds **4** were synthesized by cyclisation with suitable hydrazines of the already reported [20] β-(dimethylamino)vinyl-aldehydes **2** and **3** following our method which was further modified [21]: when hydrazine derivatives were available as hydrochlorides, they were used as such (method 1), while all the other hydrazine derivatives were made to react with equimolar quantities of hydrochloridric acid 37% (method 2).

The pyrazole derivatives have been obtained in good yields (56–76%) and in a very short period of time (**1h**). Moreover, in several cases minor amounts of the 1,3-pyrazole derivative **5** have been isolated together with the predominant 1,5-pyrazoles **4** (Scheme 1). Compound **4g** was already reported as **1f** [21]. The treatment of commercially available phenylbutenone derivatives **6** with N,N-dimethylformamide dimethyl acetal (DMFDMA) afforded the dimethylaminopentadienone intermediates **7**, as reported in the literature [22]. They in turn easily reacted with the hydrazine derivatives giving the pyrazoles **8** according to method 1 or 2. In most cases the 1,3-substituted isomers **9** were also isolated (Scheme 2).

Using the same procedure on different arylmethylketones **10** and following the synthetic routes described in the literature [23–31], we first obtained the dimethylaminopropenone intermediates **11** which cyclized with the opportune hydrazines to give the pyrazoles **12**. The 1,3-substituted isomers **13** were also isolated in seven cases. When the intermediates **11c**, **d**, **f** have a hydroxy group in ortho position, the reaction with 2-hydrazinopyridine led to the chromones **14c**, **d**, **f** probably via the intramolecular cyclization of the intermediate itself (Scheme 3) [32].

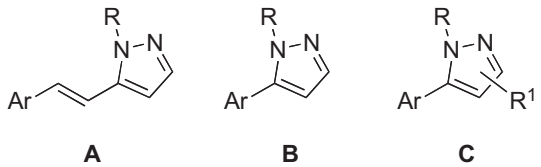

Fig. 1. General structure of new synthesized compounds.

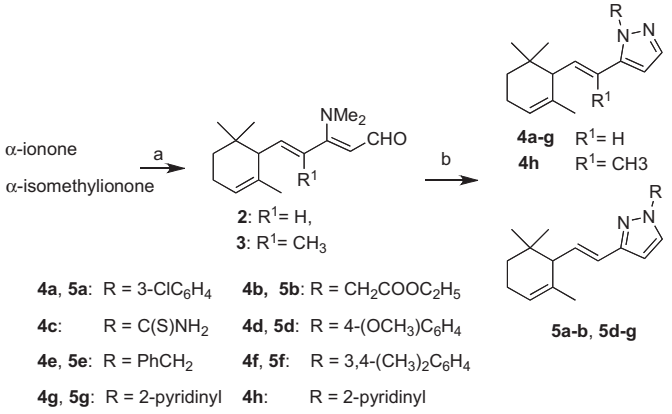

Scheme 1. Reagents and conditions: (a) Vilsmeier reaction: $POCl_3$ (50.0 mmol), N,N-dimethylformamide (3.78 mL), ionone (25.0 mmol); (b) method 1: $RNHNH_2$*HCl; method 2: $RNHNH_2$ + HCl conc.

The synthetic route followed for the synthesis of the trisubstituted pyrazoles is outlined in Schemes 4 and 5. Pyrazoles **17** were easily prepared from intermediates **16a** and **16b** which, in turn, were obtained from the commercial 1-(4-methoxyphenyl)propan-1-one **15a** and from the 1-(4-methoxyphenyl)-2-phenylethanone **15b** which was synthesized by Friedel-Crafts acylation on anisole as already reported [33]. A little amount of the isomer **18** was also isolated (Scheme 4).

The intermediate 1,3-dicarbonilyc compounds **19** and **21** were obtained by Claisen condensation between 4′-methoxyacetophenone and methyl benzoate or ethyl acetate, respectively, under nitrogen atmosphere using sodium hydride as a deprotonating agent [34,35], whereas **22** was obtained using sodium amide instead of sodium hydride. Starting from those 1,3-diketones **19**, **21**, **22** we performed the cyclisation with 2-hydrazinopyridine to pyrazoles **20**, **23**, **24**, respectively, with the same procedure described above (Scheme 5).

3. Results

3.1. Inhibition of cell proliferation

The analyses of concentration-response curves obtained from each cell line treated with our 36 compounds together with the resulting calculation of mean IC_{50}s displayed a quite broad range of sensitivity (from 0.64 ± 0.31 to more than 100 μM, Table 1). The

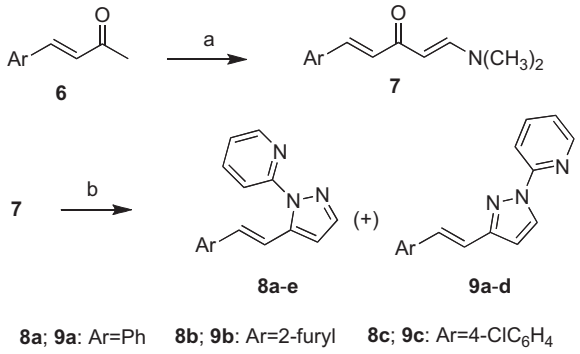

Scheme 2. Reagents and conditions: (a) DMFDMA, xylene, reflux; (b) method 1: $RNHNH_2$*HCl; method 2: $RNHNH_2$ + HCl conc.

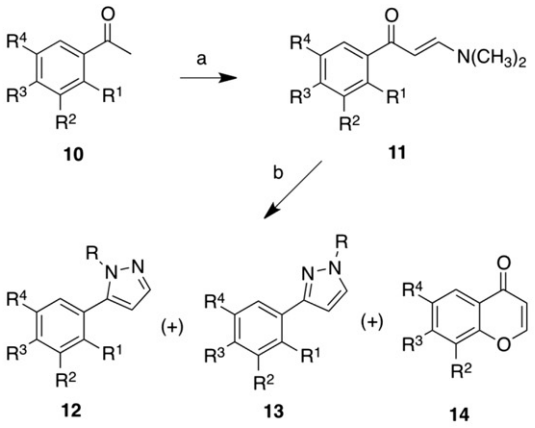

Compd	R	R^1	R^2	R^3	R^4
10a,11a	-	H	H	OCH_3	H
10b,11b	-	OH	H	H	CH_3
10c, 11c	-	OH	H	H	Cl
10d, 11d	-	OH	H	OCH_3	H
10e, 11e	-	H	H	$NHC(O)CH_3$	H
10f,11f	-	OH	H	H	H
10g, 11g	-	H	OCH_3	H	H
10h, 11h	-	H	H	morpholino	H
10i, 11i	-	OCH_3	H	OCH_3	H
10l, 11l	-	OCH_3	H	H	H
12a, 13a	2-pyridinyl	H	H	OCH_3	H
12a1, 13a1	4-chlorophenyl	H	H	OCH_3	H
12b	4-chlorophenyl	OH	H	H	CH_3
12c, 13c	2-pyridinyl	OH	H	H	Cl
12c1	4-chlorophenyl	OH	H	H	Cl
12d, 13d	2-pyridinyl	OH	H	OCH_3	H
12d1	4-chlorophenyl	OH	H	OCH_3	H
12e	2-pyridinyl	H	H	$NHC(O)CH_3$	H
12f, 13f	2-pyridinyl	OH	H	H	H
12f1	4-chlorophenyl	OH	H	H	H
12g, 13g	2-pyridinyl	H	OCH_3	H	H
12h	2-pyridinyl	H	H	morpholino	H
12i	2-pyridinyl	OCH_3	H	OCH_3	H
12l, 13l	2-pyridinyl	OCH_3	H	H	H
14c	-	H	H	H	Cl
14d	-	H	H	OCH_3	H
14f	-	H	H	H	H

Scheme 3. Reagents and conditions: (a) DMFDMA, xylene, reflux; (b) method 2: $RNHNH_2$ + HCl conc.; method 1: $RNHNH_2$*HCl.

comparison of the activities of each compound on each cell line allowed the selection of four molecules endowed with a higher activity, these compounds are: **12a**, **12a1**, **12d** and **12d1**. All these molecules were particularly active on human ovarian adenocarcinoma A2780 (**12d** > **12d1** = **12a** > **12a1**, for significant differences $p < 0.001$) and murine leukemia P388 cells (**12d** > **12a** > **12d1** > **12a1**, for significant differences $p < 0.01$). No one of our compounds showed a particularly significant activity (arbitrarily defined as ≤ 30 μM) against human lung carcinoma A549 cells (**12a** = **12d** = **12a1** = **12d1**).

3.2. Determination of apoptosis by nuclear morphological examination of cells stained by DAPI

Cell lines were then tested for the induction of apoptosis by means of DAPI staining and morphological analysis of nuclei after

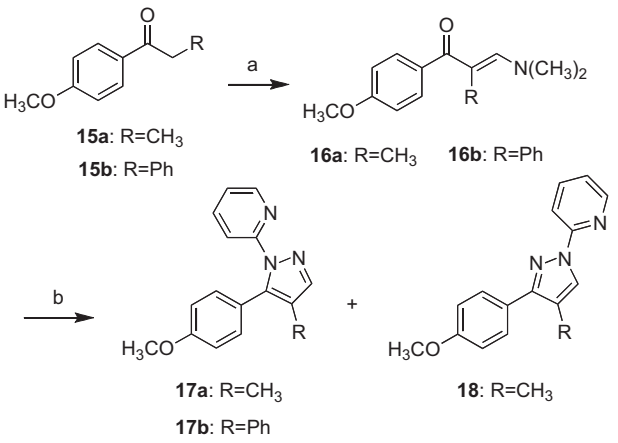

Scheme 4. Reagents and conditions: (a) DMFDMA, xylene, reflux; (b) 2-hydrazinopyridine dihydrochloride, ethanol, reflux.

exposure to equitoxic concentrations (IC_{50} and IC_{90}) of the selected compounds (Fig. 2).

On A2780 cells, **12d** showed the highest level of activity with a peak at 48 h. On A549, all molecules showed a significant level of apoptotic activity and a good concentration-response with the maximal apoptotic activity expressed at 48 h for **12d**, **12a** and **12d1**. All compounds and in particular **12a1**, showed a good level of apoptotic activity, similar or even better than that of taxol and vincristine (Fig. 2), and concentration-response on P388 cells, although with a different timing of maximal expression.

3.3. Cell cycle analysis

P388 were analyzed for the modifications of cell-cycle phases after exposure to the IC_{30} and IC_{75} of selected active substances. As shown in Table 2, our data display that in general all compounds were able to cause a partial block of cells in the G2/M phase of the cell cycle, with a concomitant decrease of cells in the S and/or G0/G1 phases, more evident after 48 h exposure. In particular, at the higher concentration and after 24 h, **12d1**, **12d** and **12a1** caused the formation of octaploid and aneuploid cells that died in the following 24–48 h.

3.4. Western blot analysis of p53, $p21^{waf1}$ and α-tubulin

To verify the involvement of **12d** in apoptotic triggering we analyzed the expression of p53 and $p21^{waf1}$ proteins both implicated in the induction of apoptosis and cell cycle arrest.

In both human cell lines **12d** was able to upregulate both molecular markers in a concentration- and time-dependent manner. The maximal effect on p53 and $p21^{waf1}$ accumulation, calculated by densitometric analysis on the basis of the relative untreated control, was observed after 24 h of treatment in A2780 cells (p53, +71% and 85% at 0.1 μM and 10 μM, respectively; $p21^{waf1}$, +42% and +62% at 0.1 μM and 10 μM, respectively, Fig. 3A) and after 72 h in A549 cells (p53, +40% and 1320% at 1 μM and 100 μM, respectively; $p21^{waf1}$, +293% and 62% at 1 μM and 100 μM, respectively, Fig. 3B).

It is also of note that the expression of α-tubulin was significantly reduced after incubation with **12d**, this effect being mostly evident in A549 cells (−37% and −94% after 72 h incubation with 10 and 100 μM for A2780 and A549, respectively). This effect could be due to the great triggering of the apoptotic activity of our compounds that necessarily involves the disruption of tubulin. This effect was in fact mostly evident after 72 h of incubation, that is when almost all the few cells alive were apoptotic and even reduced to debris.

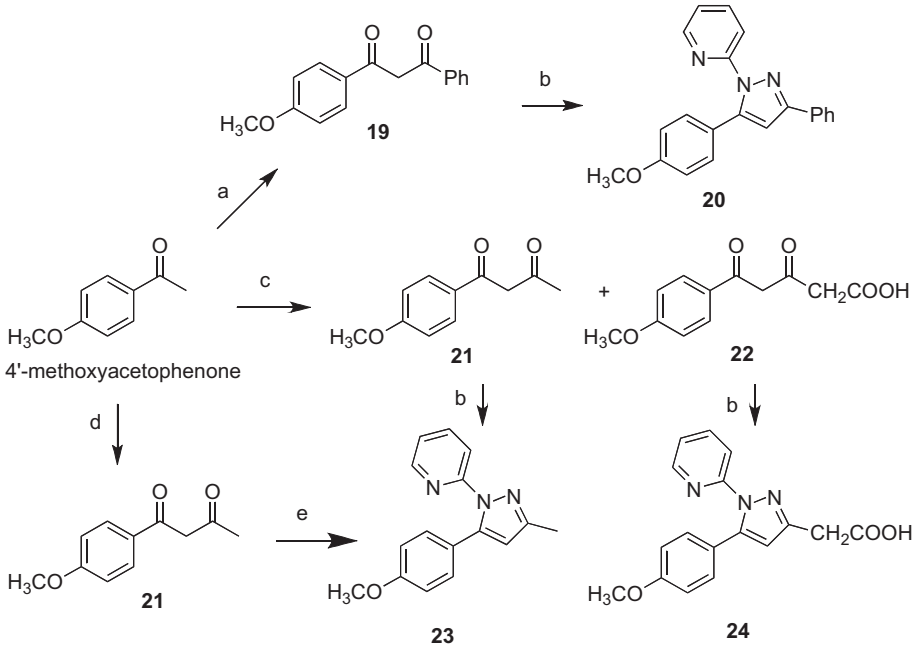

Scheme 5. Reagents and conditions: (a) $PhCOOCH_3$, NaH, toluene, reflux, N_2; (b) 2-hydrazinopyridine dihydrochloride, ethanol, reflux; (c) AcOEt, $NaNH_2$, toluene, reflux; (d) AcOEt, NaH, toluene, reflux, N_2; (e) 2-hydrazinopyridine dihydrochloride, ethanol, reflux.

3.5. *Effect of **12d** on cell microtubules*

As we observed the generation of large cells after treatment with **12d**, whose presence was also confirmed by the flow cytometry analysis, and on the basis of findings of polyploid cells in the literature concerning the effects of pyrazole compounds with anticancer activity, we hypothesized a possible involvement of the microtubule cytoskeletal system in the action mechanism of this active substance.

Therefore, we decided to study the microtubule network in A549 cells treated with **12d** by immunofluorescence microscopy. Our results are reported in Fig. 4. The compound **12d** was able to cause the condensation of microtubules into "dots" in a great percentage of cells, depending on the compound concentration applied. These "dots" were only sporadically present in control cells treated with 100 nM taxol. While typical bundles were never observed in cells treated with **12d**, these "dots" are similar to tubulin aggregates observed after treatment with colchicine and vinblastine (Fig. 4E) [36,37].

It is also of note that no other selected compound was able to cause, even at the maximal applied dose of 100 μM, the formation of these microtubule structures (data not shown).

On the basis of the immunofluorescence results we performed a docking analysis using the dimer of α- and β-tubulin as the putative target for our molecules. Docking simulation results indicated that **12d** is more likely to bind the β-tubulin in a cleft next to the interface with the α-monomer (Fig. 5), with a calculated Ki of 5.3×10^{-8} M. This compound is stabilized by hydrogen bonding to the peptidic N atom of Arg 2, the carboxylic groups of Arg 48, Leu 242 and Asn 249 and to the side chain atoms of Arg 48, Asn 50 and Asp 251 (Fig. 5A). These residues, together with Val 51 and Leu 242, form a pocket that is separated by ca. 7.0 Å from the colchicine binding site (Fig. 5B) and 10 Å from the GTP moiety bound to the α-subunit, these latter sites having been determined by X-ray crystallography [38]. Besides changing the surface characteristic at the interface of the two tubulin molecules, the presence of **12d** can interfere with residues Glu71 and Asp 98 thus altering the overall conformation of the polymer by bending the dimer (Fig. 5D). We

Table 1
IC^a_{50} as calculated by the MTT assay.

Compounds	Cell lines		
	A2780	A549	P388
4a	52.9 ± 3.0	57.1 ± 1.5	49.2 ± 5.7
4b	73.3 ± 8.1	>100	47.3 ± 13.1
4c	50.3 ± 1.5	49.3 ± 4.9	50.7 ± 4.2
4d	51.2 ± 12.6	48.4 ± 3.4	45.2 ± 13.7
4e	48.1 ± 3.0	57.8 ± 11.8	47.3 ± 3.6
4f	50.0 ± 1.6	55.8 ± 1.4	50.2 ± 3.4
4g	45.8 ± 2.6	55.8 ± 7.7	48.5 ± 1.5
4h	84.0 ± 6.4	>100	48.8 ± 3.8
8a	>100	>100	57.9 ± 7.9
8b	>100	>100	74.0 ± 14.9
8c	>100	>100	80.9 ± 19.23
8d	>100	>100	72.8 ± 5.62
8e	>100	>100	95.8 ± 17.0
12a	2.89 ± 0.72	44.7 ± 10.4	5.38 ± 0.34
12a1	5.62 ± 1.1	53.5 ± 4.7	24.2 ± 7.3
12b	50.9 ± 5.5	67.9 ± 5.8	51.7 ± 2.5
12c	>100	>100	>100
12c1	52.8 ± 3.2	>100	48.5 ± 4.1
12d	1.22 ± 0.33	52.5 ± 18.0	1.56 ± 0.42
12d1	2.35 ± 0.62	56.7 ± 15.2	7.51 ± 0.71
12e	>100	>100	>100
12f	>100	>100	>100
12f1	62.9 ± 3.7	>100	58.7 ± 7.9
12g	>100	>100	>100
12h	>100	>100	>100
12i	85.0 ± 1.8	>100	65.0 ± 7.6
12l	>100	>100	>100
13a	>100	>100	>100
13c	>100	>100	>100
13d	63.8 ± 10.4	87.1 ± 8.1	45.5 ± 6.0
13f	69.1 ± 10.6	84.5 ± 5.6	69.1 ± 10.6
13l	>100	>100	>100
17a	>100	>100	>100
17b	>100	>100	>100
20	>100	>100	62.4 ± 10.0
23	67.6 ± 5.4	>100	>100
Taxol	2.3 ± 0.8	21.5 ± 5	4.9 ± 0.4
Vincristine	ND[b]	97.8 ± 20.4	0.7 ± 0.3

[a] Mean ± SD of 3–9 experiments. Data are expressed in μM except for taxol and vincristine where they were expressed in nM.
[b] Not detected.

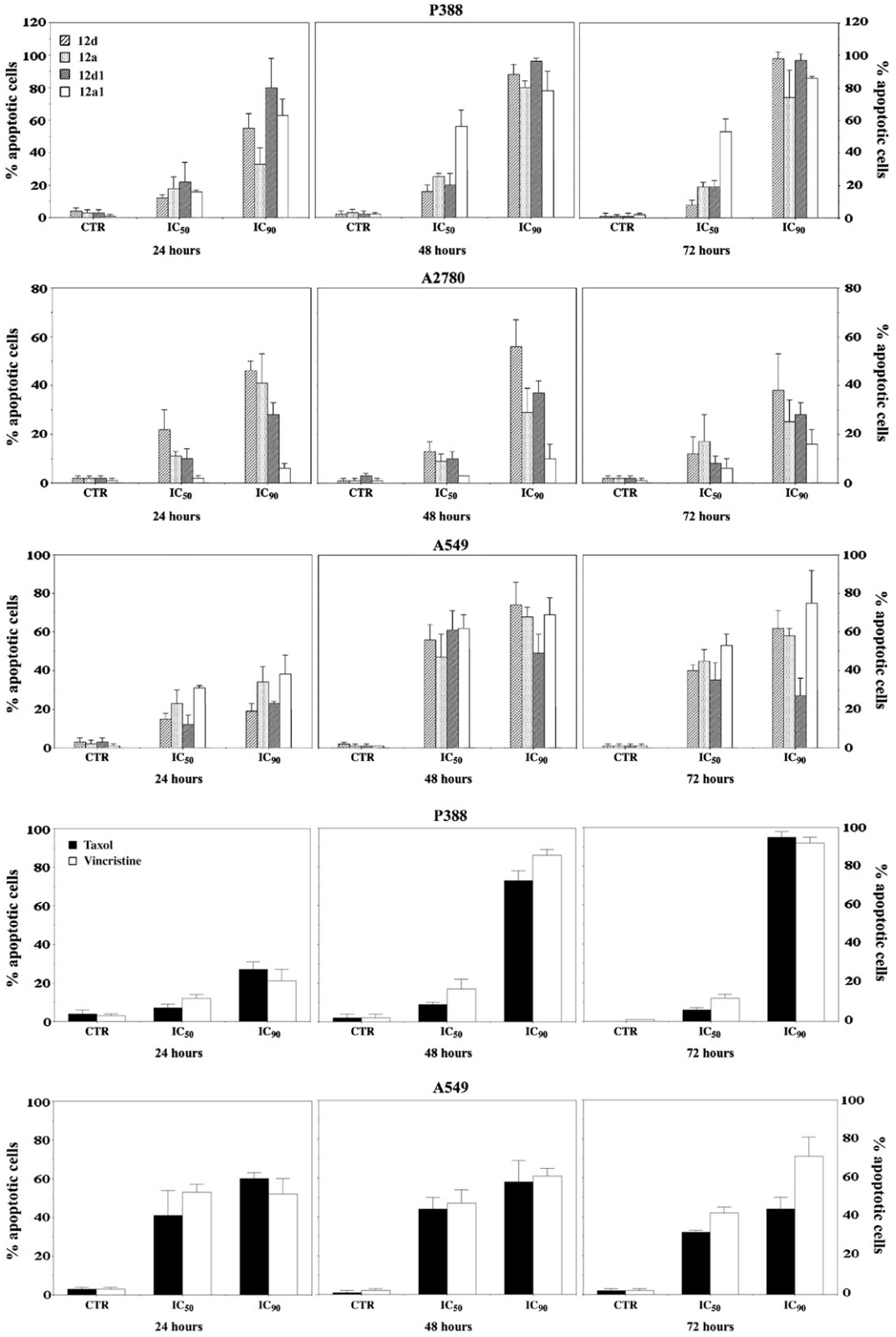

Fig. 2. Histograms represent the mean ± SD of cells treated with the IC_{50} and IC_{90} of **12a**, **12a1**, **12d**, **12d1**, taxol and vincristine and showing nuclear fragmentation, as evaluated after DAPI staining and microscopic analysis.

suggest that this bending could lead the molecular assembly to an asset similar to the one present in the tubulin–stathmin complex that does not participate in microtubule assembly. If further confirmed by crystallography, the binding site identified by our simulations would be a novel target site to use for structure-based drug design of inhibitors of tubulin polymerization (Fig. 5C).

Finally, we also tested "*in silico*" the activity and binding modes of **12a**. This molecule binds to the β-subunit in a very

Table 2
Percentage of P388 cells in the different cell-cycle phases after 24–72 hour treatment with active compounds as determined by the MTT assay.

		24 h		48 h		72 h	
		IC_{75}	IC_{30}	IC_{75}	IC_{30}	IC_{75}	IC_{30}
12a	G0/G1 (2n)	29.2 ± 1.4	31.3 ± 3.7	30.0 ± 10.9	34.7 ± 3.9	ND[a]	32.9 ± 0.6
	S	37.1 ± 5.9	48.9 ± 5.9	41.8 ± 11.4	39.7 ± 12.7	ND	49.3 ± 3.6
	G2/M (4n)	33.7 ± 5.9	19.9 ± 2.3	28.2 ± 2.5	25.6 ± 9.1	ND	17.8 ± 3.2
	Aneuploid cells	–	–	–	–	ND	–
	8n cells	–	–	–	–	ND	–
12a1	G0/G1	3.0 ± 0.9	30.4 ± 2.1	ND	34.3 ± 8.4	ND	31.7 ± 3.0
	S	32.5 ± 1.2	52.5 ± 5.4	ND	38.6 ± 14.7	ND	50.7 ± 5.1
	G2/M (4n+2n)	23.5 ± 2.8	17.2 ± 3.4	ND	27.1 ± 7.3	ND	17.6 ± 2.3
	Aneuploid ells	32.7 ± 2.0	–	ND	–	ND	–
	8n cells	8.3 ± 0.1	–	ND	–	ND	–
12d	G0/G1 (2n)	0.0	34.5 ± 0.7	ND	37.0 ± 8.6	ND	44.2 ± 1.8
	S	0.0	47.0 ± 2.7	ND	40.8 ± 15.5	ND	42.3 ± 0.4
	G2/M (4n+2n)	5.0 ± 2.0	18.5 ± 2.0	ND	22.3 ± 7.9	ND	13.4 ± 1.8
	Aneuploid cells	50.9 ± 13.5	–	ND	–	ND	–
	8n cells	44.2 ± 13.9	–	ND	–	ND	–
12d1	G0/G1 (2n)	0.0	31.0 ± 2.6	ND	34.9 ± 6.0	ND	36.4 ± 3.3
	S	0.0	50.1 ± 2.9	ND	43.0 ± 11.9	ND	46.3 ± 6.3
	G2/M (4n+2n)	9.2 ± 4.1	18.8 ± 0.9	ND	22.1 ± 6.3	ND	17.3 ± 3.2
	Aneuploid cells	56.6 ± 14.9	–	ND	–	ND	–
	8n cells	34.2 ± 16.9	–	ND	–	ND	–
Taxol	G0/G1 (2n)	8.2 ± 0.6	7.3 ± 0.1	21.5 ± 1.8	20.1 ± 5.2	15.5 ± 1.7	13.5 ± 2.8
	S	24.3 ± 6.6	36.2 ± 11.4	24.7 ± 1.0	25.9 ± 3.9	25.3 ± 2.3	27.1 ± 2.7
	G2/M (4n+2n)	67.7 ± 5.9	56.6 ± 11.5	7.4 ± 1	8.5 ± 1.3	18.6 ± 0.8	17.3 ± 2.9
	Aneuploid cells	–	–	35.9 ± 6.5	38.2 ± 3.6	38.2 ± 1.6	40.0 ± 2.6
	8n cells	–	–	10.6 ± 6.3	7.5 ± 3.5	2.5 ± 0.2	2.2 ± 0.1
Vincristine	G0/G1 (2n)	29.8 ± 5.1	32.5 ± 6.7	10.3 ± 1.6	25.3 ± 1.5	11.9 ± 2.7	23.1 ± 0.2
	S	52.3 ± 16.3	52.0 ± 10.8	29.0 ± 3.5	57.8 ± 3.9	29.6 ± 2.8	61.1 ± 0.5
	G2/M (4n+2n)	18.0 ± 11.2	12.4 ± 5.5	32.3 ± 13.2	17.0 ± 2.4	24.0 ± 3.5	15.9 ± 0.7
	Aneuploid cells	–	–	26.4 ± 9.9	–	32.7 ± 4.0	–
	8n cells	–	–	2.1 ± 1.4	–	1.9 ± 0.6	–
		24 h		48 h		72 h	
CTR	G0/G1 (2n)	33.2 ± 3.1		31.6 ± 7.6		36.6 ± 8.5	
	S	8.6 ± 3.2		52.0 ± 9.5		49.9 ± 9.3	
	G2/M (4n)	18.2 ± 2.0		16.4 ± 2.8		13.6 ± 2.2	

[a] ND, not detected due to the low number of evaluable alive cells. Mainly apoptotic cells were still present.

similar way to **12d** but with a much weaker affinity constant (Ki ca. 1.8×10^{-6}).

3.6. *Effect of **13d** and **12d1** on microtubules*

Docking simulations performed on the two moieties tested led to similar results. Both molecules in fact showed a similar fitness function and a similar predicted Ki (using GOLD and Autodock respectively) with a very favorable clusterization of the results. Structurally, the simulation results indicated that the inactive isomer **13d** is more likely to bind the β-tubulin, within a cleft close to the interface between the two protomers but without a direct interaction with the α-subunit (see Fig. 5A). **13d** is stabilized by hydrogen bonding to the carboxylic group of Asn 258 and to the side chain atoms of Asn 249, Lys 254 and Asn 258. The hydrophobic residues Leu 248, Ala 250, Leu 252, Leu 255 and Met 259 contribute to form the pocket containing the colchicine binding site. However, the smaller **13d** resulted inactive on tubulin probably because colchicine is able to interact both with the β-subunit and with residues belonging to the molecule, whilst **13d** is located more deeply in the β-subunit. On the other side, **12d1** is perfectly superpositioned on the **12d** as the docking simulations showed. The presence of a chlorine in para-position confers to **12d1** the ability to interact with β-tubulin, possibly forming an alogen bond with the carboxylic group of Leu 255 of this molecule, however, the same atom can also interact with the hydrophobic residues since the interaction of **12d1** (predicted Ki of 1.8×10^{-6} M) to the tubulin dimer is less favorable than that of **12d**.

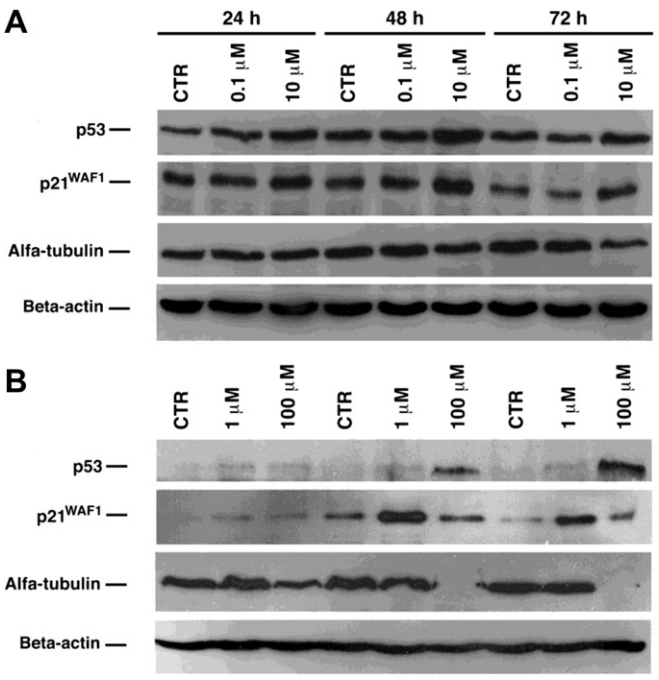

Fig. 3. Western blot of p53 and $p21^{waf1}$ and α-tubulin after exposure for 24–72 h of A2780 (A) and A549 (B) cells to 0.1 and 10 μM and to 1 and 100 μM **12d**, respectively. Note both the upregulation with the maximal expression after 48 h of both apoptosis and cell cycle arrest markers and the reduction of α-tubulin bands after exposure to high concentrations of **12d**, in particular in A549 cells. Beta-actin was used for the densitometric normalization. Prestained molecular markers were always included as reference.

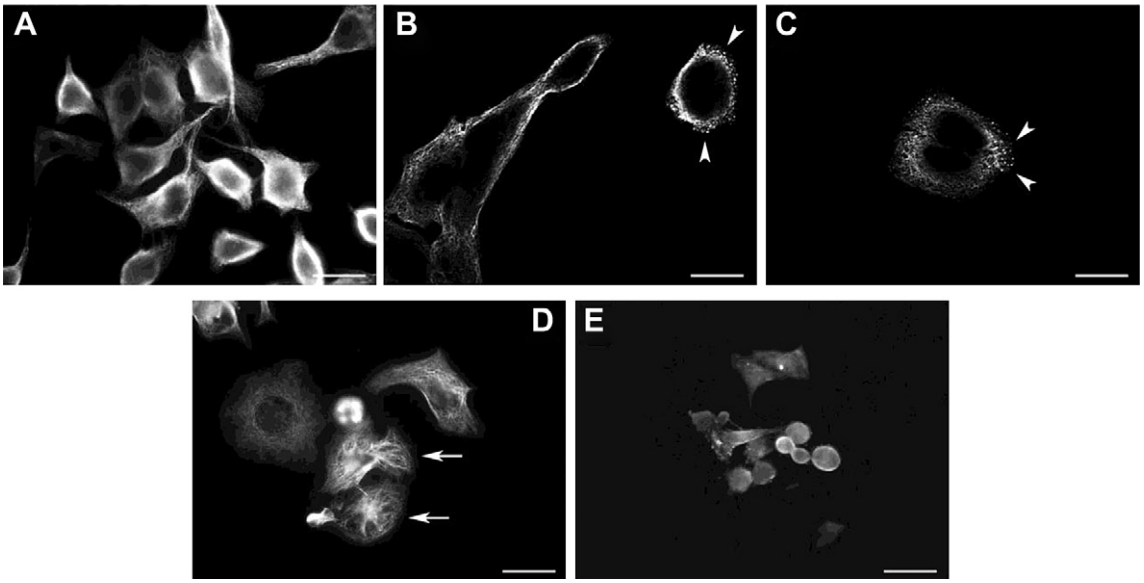

Fig. 4. Microtubular effect of **12d** in A549 cells. Panel A: Untreated control cells. Panel B and C: Cells treated with 10 and 100 μM **12d**, respectively. Note the formation of many round microstructures, as indicated by the arrowheads. Panel D: A549 cells treated with 100 nM taxol and showing typical bundles, as indicated by the arrows. Panel E: A549 cells treated with 25 nM vinblastine. Note the round microstructure in some cells interpreted as tubulin aggregates. Bar = 20 μm (A–D). Bar = 31.5 μm (E).

3.7. Tubulin polymerization assay

In order to investigate the possible involvement of microtubule cytoskeleton in the action mechanism of the active compounds, we examined the effect of **12a**, **12a1**, **12d**, and **12d1** on microtubule polymerization using an in vitro assay. An increase in the absorbance at 460 nm indicates an increase in tubulin polymerization (Fig. 6A). As expected, taxol gave an increase in absorbance above

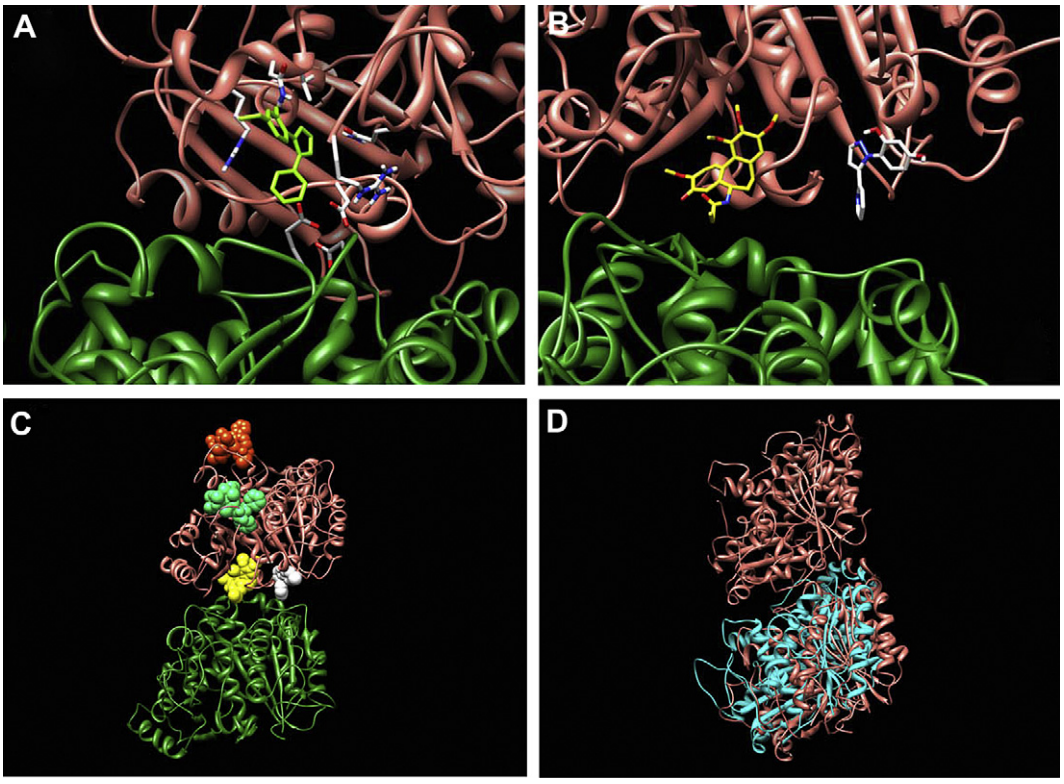

Fig. 5. *Panel A*: The interface between α (green) and β (salmon) subunits. The **12d** moiety position, as determined by docking simulation, is reported in light green. Residues involved in ligand binding are drawn as sticks. *Panel B*: **12d** predicted binding site is displaced by ca. 7 Å from the colchicine binding site, this latter as determined by X-ray crystallography. However both the molecules interfere with residues in loop Leu 242–Arg 250 of β-tubulin. *Panel C*: Identification of at least four different binding sites in β-tubulin (salmon ribbons) three-dimensional structure: **12d** (white) and colchicine (yellow) bind at the interface between the α (dark green) and β (salmon) subunits, taxol (light green) binds on the β-subunit surface, vinblastine (orange) on the β:α dimeric interface. *Panel D*: In salmon the structural arrangement of α:β dimer bound to **12d**. In cyan the α-subunit in the native position (pdb code 1JFF). (For interpretation of the references to colour in this figure legend, the reader is referred to the web version of this article.)

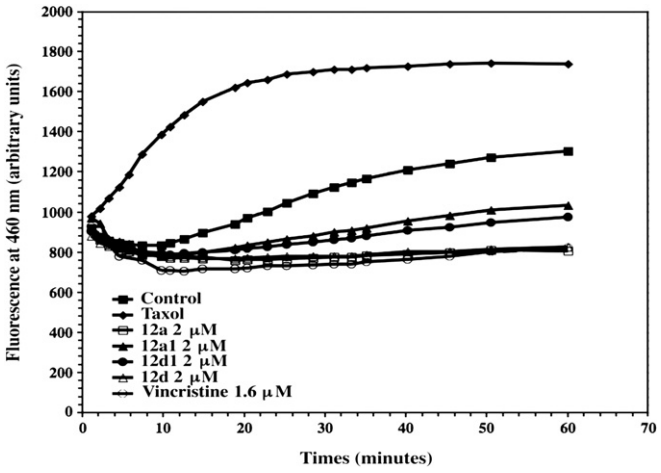

Fig. 6. In vitro tubulin polymerization assay. Porcine brain tubulin polymerization was measured in absence (Control, 4% DMSO) or in presence of 3 μM Taxol, 1.6 μM Vincristine, and **12a**, **12a1**, **12d** and **12d1** compounds at 2 μM concentation.

the control: in contrast, 1.6 μM vincristine strongly inhibits microtubule polymerization. Tested compounds showed a trend similar to vincristine, suggesting that they destabilize microtubules (Fig. 6), although they did not show significant differences in terms of their concentrations inhibiting 50% polymerization that reasonably was much higher than that of vincristine in our test conditions (IC_{50}s: 1.48 ± 0.01, 1.78 ± 0.03, 1.64 ± 0.03 and 1.46 ± 0.07 μM for **12a**, **12a1**, **12d1** and **12d**, respectively, vincristine < 1.6 μM).

4. Discussion and conclusions

In the last decades pharmacological research has been strongly devoted to in the discovery of new conventional and target-based anticancer drugs with the aim of finding drugs with new mechanisms of action, possibly involving new molecular pathways, with a spectrum of activity toward those tumors with lower responsiveness and high mortality, and with the ability to overcome the most common mechanisms of resistance. On this basis we undertook the present study analyzing 36 new pyrazole derivatives for their ability to inhibit tumor cell growth.

The preliminary screening on human ovarian adenocarcinoma A2780, murine leukemia P388 and human lung carcinoma A549 cell lines evidenced a great difference in activity strictly related to the pyrazole substituents. The presence of the cyclohexenylvinyl moiety yielded compounds (**4**) showing an antiproliferative activity in all the cell lines tested only at concentrations greater than 50 μM. The substitution of the cyclohexenylvinyl with an aryl moiety caused a decrease of activity (see compd. **8**), while the further removal of the vinyl linker greatly enhanced the antiproliferative activity. In fact, compounds **12** were the most active out of all those synthesized. It is worth noting that all the 1,3-substituted pyrazoles **5** [21] and **13** (see Table 1) were inactive or showed a dramatic loss of potency. Further SAR considerations can be made by observing which substituents gave the most active compounds in the **12** series. Firstly, the best substituent in position 1 is the 2-pyridinyl moiety, since all the 4-chlorophenyl substituted were less active or inactive (compare compd. **12d** and **12d1**). Moreover, the phenyl substituents R^1 and R^3 played a fundamental role in determining the potency of the activity. In particular, when both OH and OCH_3 groups were present or R^3 was OCH_3, we obtained the most active compounds **12d** and **12a**. All the other aryl substituents, in spite of the presence of the 2-pyridinyl moiety, gave inactive compounds (see **12e**-**12l**).

We thus selected the four active compounds (**12d**, **12d1**, **12a** and **12a1**) and confirmed their pro-apoptotic activity along with their significant antiproliferative activity, although the latter was observed in the micromolar range of IC_{50} instead of the nanomolar range, as occurs with more classical antimicrotubule agents such as taxol and vincristine.

Apoptosis was induced at a different extent, with respect to the time of exposure and the concentrations used for each compound and it was confirmed for **12d** in human cells by western blot analysis of two markers of apoptosis and cell cycle arrest such as p53 and $p21^{waf1}$. In particular, in A549 cells the apoptotic activity of our compounds appeared to be higher than expected on the basis of the IC_{50} for the antiproliferative activity (see Table 1 and Fig. 2). Nevertheless, these results are not in contrast since we treated our cells at equitoxic conditions, i.e. with compound IC_{50}s and IC_{90}s. Once disconnected from the applied absolute concentrations applied, these results suggested that the triggering of apoptotic activity was the prevalent killing mechanism of our active compounds, a fortiori if we consider the final lower antiproliferative activity on A549 cells. On the other hand both taxol and vincristine, used here as controls, showed a similar apoptotic activity in spite of their much lower applied IC_{50} and IC_{90}.

The analysis of the cell cycle phases showed a block of cells in the G2/M phase with a concomitant decrease in the S and/or G0/G1 phases. In particular, after 24 h exposure to the IC_{75}s, cells in S or G0/G1 phases were slightly lower (see **12a**) or absent (**12d1**, **12d** and **12a1**) compared to controls, in this case this was due to the appearance of abnormal cell cycles and the formation of polyploid/aneuploid cells. In fact, after the first 24 h, P388 cells exposed to the IC_{75} of **12d1**, **12d** and **12a1** compounds became unable to proceed through the normal phases of mitosis due to their polyploidy and died in the following 24–48 h generating a great number of cell debris and a culture containing mainly apoptotic cells. After 48 h cells exposed to the compound IC_{30}s showed a more or less marked reduction of cells in the S phase of the cell cycle along with a relative increase of G2/M cells. If compared to classical antimicrotubule drugs, such as vincristine and taxol, our compounds show a much greater propensity to cause accumulation of aneuploid/polyploid cells.

The results of cell cycle analysis, the simple microscopic observation of quite large cells and, finally, the observation of others [39–42] that antiproliferative pyrazole compounds were often able to inhibit tubulin polymerization through a binding site interaction, similar in part to that of colchicine, suggested the possibility of a mechanism of action directly or indirectly involving the microtubular system.

Therefore, we chose to perform a microscopic analysis of the microtubular cytoskeletal system, a docking analysis, and a tubulin polymerization assay to verify the ability of our compounds to interact with microtubules.

The immunofluorescence microscopy of the microtubule network revealed that **12d** caused a complete breakdown of microtubules with the formation of “dots” similar to the tubulin aggregates observed after treatment with microtubule disaggregating agents such as colchicine and vinblastine [36,37]. The microscopic observations were also in agreement with results obtained by western blot analysis for **12d**. In fact, a partial or complete reduction of α-tubulin was clearly observed and correlated with **12d** concentration and time of exposure. Furthermore, **12d** did not cause the formation of bundles or other similar structures, which are observed after treatment with taxol, and none of the other active compounds tested (**12d1**, **12a** and **12a1**) caused microtubular structures similar to aggregates or bundles, also at high concentrations.

Due to its antiproliferative and pro-apoptotic activities and its apparent peculiarity as microtubule-interfering agent, **12d** was then docked against the α-β dimer of tubulin and compared to the inactive **13d** and to the active compounds **12d1** and **12a**, in order to verify a possible interaction with this target and its molecular features. Our results indicated that **12d** may interfere with the regular microtubule formation because of its ability to form a bridge between α and β-subunits. This probably greatly disturbs the regular curvature of the tubulin complex and thus the correct growth of the microtubule during polymerization giving prevalence to the phenomena of depolymerization. This aspect could also explain the formation of the "dots" observed by microscope. Furthermore, on the basis of the docking analysis we also can draw out that, similarly to **12d**, **12d1** is more likely to interfere with the regular microtubule formation with respect to **13d**, because of its ability to form a bridge between the two subunits, also in this case disturbing the regular curvature of the tubulin complex in this case as well. On the other hand, this interaction had a predicted Ki 10 times higher than that of **12d**, which in part may justify the absence of microtubule breakdown by this compound as revealed by immunofluorescence, also after exposure to high concentrations. Similarly, and in spite of its depolymerizating activity, which was similar to that of **12d** as shown by our specific cell free polymerization assay, **12a** did not show a great activity in our docking system. This together with the absent activity at the microscope analysis were the reasons why we preferred to focus our efforts on **12d**.

Although all our results obtained by docking analysis should be confirmed by crystallography, the most important result of this *in silico* study is that the binding site identified by our simulations would be a novel target site to use for structure-based drug design of inhibitors of tubulin polymerization and different from those already described for other pyrazole microtubule interfering agents and anticancer drugs such as taxol, colchicine, vincristine and other related compounds. On the other hand our data do not completely exclude the hypothesis of other targets for our compounds. In particular, the presence of a high percentage of polyploid/aneuploid cells makes our compounds similar in behavior to aurora inhibitors [43,44]. These compounds, some of which are in clinical phases of study [44], are able to inhibit the activity of aurora kinases blocking the correct development of the various phases of mitosis such as the centrosome separation, the mitotic entry, the spindle assembly, the correct alignment of chromosomes and cytokinesis. Alternatively, our compounds could inhibit the activity of γ tubulin, a further component of the centrosome and spindle pole bodies [45,46], whose inactivation may stimulate polyploidization. For both targets we applied docking simulations whose results showed a very low probability of binding of our compounds to the possible target sites of aurora kinase and γ tubulin, with Ki ranging in the micromolar range of concentrations.

In conclusion, very important indications emerge from the biological investigations on these new pyrazole derivatives. In fact, in spite of their lower antiproliferative activity, compared to the more classic antimicrotubule anticancer compounds such as taxol or vincristine, our new pyrazole compounds are likely to bind to the possible newly described target site on microtubules and represent the rational for the future development of new small molecules acting as tubulin polymerization inhibitors potentially useful as anticancer drugs.

5. Experimental section

5.1. Chemistry

The purity of all the compounds was checked by thin-layer chromatography on silica gel 60-F-254 pre-coated plates and the spots were located in UV light or by vanillin in sulfuric acid. Melting points were obtained with a Fisher-Johns apparatus and are uncorrected. IR spectra were recorded with a Perkin–Elmer 398 spectrometer in film or KBr disks. ^{1}H and ^{13}C NMR spectra were determined with a Varian Gemini 200 (200 MHz, ^{1}H; 50 MHz, ^{13}C) or a Bruker DPX 300 (300 MHz) instrument, in $CDCl_3$ or (D_6)DMSO; chemical shifts (δ) are given in part per million from the peak of tetramethylsilane as internal standard; coupling constants (J) in Hz. Elemental analyses: Carlo Erba 1106 Elemental Analyser. Microanalysis of all synthesized compounds agreed within ± 0.3% of calculated values. CG-MS analyses: HP 6890–5973, GC parameters: injector temperature 250 °C; HP5 poly(methylphenilsyloxane) column 30 m, 0.25 mm, 0.25 μm; temperature profile: from 100 to 300 °C; 10 °C/min; MS parameters mode SCAN 40–600 amu.

5.1.1. 3-Dimethylamino-4-methyl-5-(2,6,6-trimethyl-1-cyclohexen-1-yl)-2,4-pentadienal (**3**)

Phosphorous oxychloride (50.0 mmol; 4.57 mL) was added dropwise, within 15 min at 0 °C, to 3.87 mL of N,N-dimethylformamide in a two-necked flask protected from atmospheric moisture and efficiently stirred with a magnetic bar. A solution of α-isomethylionone (25.0 mmol) in 3 mL of dimethylformamide was dropped into the above Vilsmeier reagent, cooled at −20 °C left to stir while the temperature was left to rise to 0 °C for a total of 45 min and finally poured onto crushed ice. The aqueous layer was alkalinized with NaOH 2N, stirred overnight and then extract with $CHCl_3$. The organic layers were combined, washed with water, dried over sodium sulfate, and evaporated at reduced pressure to give the crude product. It was purified by silica gel chromatography using AcOEt as eluant. The white solid was crystallized from AcOEt, mp. 80–81 °C. Yield 53%. IR (KBr): ν 2961, 2921, 1626, 1548, 1379, 1181 cm^{-1}; ^{1}H NMR (200 MHz, $CDCl_3$): δ 0.81 (3H, s, CH_3), 0.93 (3H, s, CH_3), 1.20–1.24 (1H, m, H-5′), 1.41–1.45 (1H, m, H-5′), 1.61 (3H, s, CH_3), 1.92 (3H, s, CH_3), 1.97–1.99 (2H, m, H-4′), 2.52–2.55 (1H, m,, H-1′), 2.92 (6H, s, NCH_3), 5.11 (1H, d, CH-2, J = 8.6 Hz), 5.30–5.36 (2H, m, H-4′ + CH-5), 9.16 (1H, d, CHO, J = 8.6 Hz); ^{13}C NMR (50 MHz, $CDCl_3$): δ 16.6 (CH_3), 22.3 (CH_3); 22.4 (CH_2); 26.2 (CH_3); 26.7 (CH_3); 30.3 (CH_2); 31.9 (C); 48.4 ($2CH_3$); 100.4 (CH); 120.7 (CH), 128.1 (C), 132.4 (CH), 136.4 (C), 170.9 (C), 189.3 (C). Anal. calcd. for $C_{16}H_{25}NO$: C, 77.68; H, 10.19; N, 5.66; found: C, 77.81; H, 10.15; N, 5.31.

5.1.2. General procedure for cyclization to pyrazole from enamines

The hydrazines (method 2) or hydrazine hydrochlorides (2 mmol) (method 1) were added in one portion to a stirred solution of enammines (2 mmol) in acidified ethanol (10 mL containing 0.17 mL of HCl 37%) (method 2) or ethanol (10 mL) (method 1). The resulting solution was stirred for different time at different temperatures. After cooling, several compounds were collected from the reaction mixture by filtration and then crystallized; other compounds were obtained by silica gel chromatography of the residue after removal of the solvent.

*5.1.2.1. 1-(3-chlorophenyl)-5-(2,6,6-trimethyl-2-cyclohex-1-yl) ethenyl-1H-pyrazole (**4a**); 1-(3-chlorophenyl)-3-(2,6,6-trimethyl-2-cyclohex-1-yl)ethenyl-1H-pyrazole (**5a**).* From 3-chlorophenylydrazine hydrochloride at 25 °C for 1 h (method 1). After evaporation to dryness, the residue was chromatographed on silica gel eluting with toluene. The first eluate gave **5a** as a red thick oil. Yield 16%. The second eluted gave **4a** as a red thick oil. Yield 64%. Data of **4a**: IR (film): ν 2957, 2915, 1595,1488, 1433 cm^{-1}; ^{1}H NMR (200 MHz, $CDCl_3$): δ 0.88 (3H, s, CH_3), 0.91 (3H, s, CH_3), 1.28–1.33 (1H, m, H-5′), 1.41–1.48 (1H, m, H-5′), 1.60 (3H, s, CH_3), 2.00–2.04 (2H, m, H-4′), 2.23 (1H, d, J = 8.2, H-1′), 5.04–5.03 (1H, m, H-3′), 6.10 (1H, dd, J = 8.2; 15.6, ethene), 6.18 (1H, d, J = 15.6, ethene), 6.45 (1H, d,

J = 1.8, H-4), 7.36–7.50 (4H, m, Ar), 7.59 (1H, J = 1.8, H-3). Anal. calcd. for $C_{20}H_{23}ClN_2$: C, 73.49; H, 7.09; N, 8.57; Cl, 10.85; found: C, 73.52; H, 7.02; N, 8.50.

Data of **5a**: IR (film): ν 2961, 2915, 1595,1488, 1447 cm^{-1}; ^1H NMR (200 MHz, $CDCl_3$): δ 0.89 (3H, s, CH_3), 0.90 (3H, s, CH_3), 1.18–1.23 (1H, m, H-5′), 1.42–1.48 (1H, m, H-5′), 1.63 (3H, s, CH_3), 2.01–2.05 (2H, m, H-4′), 2.27 (1H, d, J = 9.4, H-1′), 5.43–5.45 (1H, m, H-3′), 6.14 (1H, dd, J = 9.4, 16.0, ethene), 6.48 (1H, d, J = 16.0, ethene), 6.54 (1H, d, J = 2.6, H-4), 7.20–7.38 (2H, m, Ar), 7.52–7.53 (1H, m, Ar), 7.71 (1H, *t*, J = 2.0, Ar), 7.82 (1H, J = 2.6, H-5). Anal. calcd. for $C_{20}H_{23}ClN_2$: C, 73.49; H, 7.09; N, 8.57; Cl, 10.85; found: C, 73.59; H, 7.05; N, 8.42.

*5.1.2.2. Ethyl 2-{5-[2-(2,6,6-trimethylcyclohexen-2-yl)vinyl]-1H-pyrazol-1-yl}ethanoate (**4b**), ethyl 2-{3-[2-(2,6,6-trimethylcyclohexen-2-yl)vinyl]-1H-pyrazol-1-yl}ethanoate (**5b**).* From ethyl hydrazine hydrochloride at 50 °C for 1 h (method 1 – see ref. [21]).

*5.1.2.3. 5-(2,6,6-Trimethyl-2-cyclohexen-1-yl)ethenyl-1H-pyrazole-1-thiocarboxamide (**4c**).* From thiosemicarbazide at reflux for 1 h (method 2). After evaporation to dryness, the residue was chromatographed on silica gel eluting with toluene. The eluate gave **4c** as an already pure yellow crystals, mp 80–82 °C. Yield 76%. IR (film): ν 3252, 3150, 2958, 2915, 1590, 1495, 1247 cm^{-1}; ^1H NMR (200 MHz, $CDCl_3$): δ 0.86 (3H, s, CH_3), 0.93 (3H, s, CH_3), 1.19–1.23 (1H, m, H-5′), 1.41–1.48 (1H, m, H-5′), 1.61 (3H, s, CH_3), 2.00–2.05 (2H, m, H-4′), 2.26 (1H, d, J = 8.5, H-1′), 5.44–5.46 (1H, m, H-3′), 6.22 (1H, dd, J = 8.5; 15, ethene), 6.34 (1H, d, J = 15, ethene), 6.49 (1H, d, J = 2.8, H-4), 6.84 (1H, s, NH), 8.26 (1H, s, NH), 8.55 (1H, d, J = 2.8, H-3). Anal. calcd. for $C_{15}H_{21}N_3S$: C, 65.41; H, 7.69; N, 15.26; found: C, 65.64; H, 7.91; N, 15.02.

*5.1.2.4. 1-(4-methoxyphenyl)-5-(2,6,6-trimethyl-2-cyclohex-1-yl) ethenyl-1H-pyrazole (**4d**); 1-(4-methoxyphenyl)-3-(2,6,6-trimethyl-2-cyclohex-1-yl)ethenyl-1H-pyrazole (**5d**).* From 4-methoxyphenylhydrazine hydrochloride at 50 °C for 1 h (method 1). After evaporation to dryness, the residue was chromatographed on silica gel eluting with toluene. The first eluate gave **5d** as a yellow thick oil. Yield 17%. The second eluted gave **4d** as a yellow thick oil. Yield 67%. Data of **4d**: IR (film): ν 2958, 2913, 1515, 1250 cm^{-1}; ^1H NMR (200 MHz, $CDCl_3$): δ 0.85 (3H, s, CH_3), 0.89 (3H, s, CH_3), 1.17–1.21 (1H, m, H-5′), 1.38–1.44 (1H, m, H-5′), 1.57 (3H, s, CH_3), 1.99–2.03 (2H, m, H-4′), 2.19 (1H, d, H-1′ J = 8.3 Hz), 3.85 (3H, s, CH_3), 5.41–5.43 (1H, m, H-3′), 6.01 (1H, dd, ethene, J = 8.3; 15.8 Hz), 6.16 (1H, d, ethene, J = 15.8 Hz), 6.44 (1H, d, H-4, J = 2.0 Hz), 6.97 (2H, d, J = 8.6 Hz, Ar), 7.36 (2H, d, J = 8.6 Hz, Ar), 7.57 (1H, d, H-3, J = 2.0 Hz). Anal. calcd. for $C_{21}H_{26}N_2O$: C, 78.22; H, 8.13; N, 8.69; found: C, 77.91; H, 8.31; N, 8.74. Data of **5d**: IR (film): ν 2959, 2914, 1524, 1256 cm^{-1}; ^1H NMR (200 MHz, $CDCl_3$): δ 0.88 (3H, s, CH_3), 0.93 (3H, s, CH_3), 1.17–1.22 (1H, m, H-5′), 1.42–1.50 (1H, m, H-5′), 1.63 (3H, s, CH_3), 2.01–2.04 (2H, m, H-4′), 2.27 (1H, d, J = 8.9,, H-1′), 3.83 (3H, s, CH_3), 5.43–5.45 (1H, m, H-3′), 6.12 (1H, dd, J = 8.9; 16.6, ethene), 6.48 (1H, d, J = 16.6, ethene), 6.50 (1H, d, J = 2.4, H-4), 6.94 (2H, d, J = 9.0, Ar), 7.56 (2H, d, J = 9.0, Ar), 7.72 (1H, d, J = 2.4, H-5). Anal. calcd. for $C_{21}H_{26}N_2O$: C, 78.22; H, 8.13; N, 8.69; found: C, 77.87; H, 8.44; N, 8.69.

*5.1.2.5. 1-Benzyl-5-(2,6,6-trimethyl-2-cyclohex-1-yl)ethenyl-1H-pyrazole (**4e**); 1-benzyl-3-(2,6,6-trimethyl-2-cyclohex-1-yl)ethenyl-1H-pyrazole (**5e**).* From benzylhydrazine dihydrochloride at reflux for 1 h (method 1). After evaporation to dryness, the residue was chromatographed on silica gel eluting with toluene. The first eluate gave **5e** as a white solid, mp 73–74 °C. Yield 28%. The second eluted gave **4e** as a yellow oil. Yield 56%. Data of **4e**: IR (film): ν 2958, 2917, 1455, 1400 cm^{-1}; ^1H NMR (200 MHz, $CDCl_3$): δ 0.76 (3H, s, CH_3), 0.86 (3H, s, CH_3), 1.14–1.19 (1H, m, H-5′), 1.35–1.41 (1H, m, H-5′), 1.47 (3H, s, CH_3), 1.98–2.02 (2H, m, H-4′), 2.19 (1H, d, H-1′, J = 8.7 Hz), 5.39 (2H, s, CH_2), 5.41–5.43 (1H, m, H-3′), 6.00 (1H, dd, J = 8.7, 15.2, ethene), 6.18 (1H, d, J = 15.2, ethene), 6.34 (1H, d, J = 2.2, H-4), 7.07–7.29 (5H, m, Ar), 7.47 (1H, d, H-3, J = 2.2 Hz). Anal. calcd. for $C_{21}H_{26}N_2$: C, 82.31; H, 9.14; N, 8.55; found: C, 82.25; H, 8.94; N, 8.65. Data of **5e**: IR (KBr): ν 2967, 2953, 2906, 1451, 1050 cm^{-1}; ^1H NMR (200 MHz, $CDCl_3$): δ 0.87 (3H, s, CH_3), 0.92 (3H, s, CH_3), 1.17–1.22 (1H, m, H-5′), 1.42–1.47 (1H, m, H-5′), 1.62 (3H, s, CH_3), 1.99–2.03 (2H, m, H-4′), 2.24 (1H, d, H-1′ J = 9.5 Hz), 5.27 (2H, s, CH_2), 5.41–5.43 (1H, m, H-3′), 6.02 (1H, dd, ethene, J = 9.5, 16.0 Hz), 6.33 (1H, d, H-4, J = 2.4 Hz), 6.40 (1H, d, ethene, J = 16.0 Hz), 7.21–7.34 (6H, m, Ar + H-5). Anal. Calcd. for $C_{21}H_{26}N_2$: C, 82.31; H, 9.14; N, 8.55; found: C, 82.29; H, 8.99; N, 8.60.

*5.1.2.6. 1-(3,4-dimethylphenyl)-5-(2,6,6-trimethyl-2-cyclohex-1-yl) ethenyl-1H-pyrazole (**4f**); 1-(3,4-dimethylphenyl)-3-(2,6,6-trimethyl-2-cyclohex-1-yl)ethenyl-1H-pyrazole (**5f**).* From 3,4-dimethylphenylydrazine hydrochloride at 50 °C for 1 h (method 1). After evaporation to dryness, the residue was chromatographed on silica gel eluting with toluene. The first eluate gave **5f** as thick yellow oil. Yield 15%. The second eluated gave **4f** as a thick yellow oil. Yield 60%. Data of **4f**: IR (film): ν 2957, 2917, 1670, 1613, 1507, 1449, 1383 cm^{-1}; ^1H NMR (200 MHz, $CDCl_3$): δ 0.87 (3H, s, CH_3), 0.90 (3H, s, CH_3), 1.18–1.23 (1H, m, H-5′), 1.40–1.48 (1H, m, H-5′), 1.59 (3H, s, CH_3), 1.99–2.04 (2H, m, H-4′), 2.20 (1H, d, J = 8.8, H-1′), 2.30 (3H, s, CH_3), 2.31 (3H, s, CH_3), 5.40–5.43 (1H, m, H-3′), 6.03 (1H, dd, J = 8.8; 15.6, ethene), 6.19 (1H, d, J = 15.6, ethene), 6.44 (1H, d, H-4, J = 2.0 Hz), 7.19–7.25 (3H, m, Ar), 7.58 (1H, d, J = 2.0, H-3). Anal. calcd. for $C_{22}H_{28}N_2$: C, 82.45; H, 8.81; N, 8.74; found: C, 82.33; H, 8.97; N, 8.84. Data of **5f**: IR (film): ν 2959, 2919, 1670, 1613, 1518, 1454, 1381 cm^{-1}; ^1H NMR (200 MHz, $CDCl_3$): δ 0.89 (3H, s, CH_3), 0.94 (3H, s, CH_3), 1.9–1.24 (1H, m, H-5′), 1.44–1.53 (1H, m, H-5′), 1.63 (3H, s, CH_3), 2.01–2.06 (2H, m, H-4′), 2.26 (3H, s, CH_3), 2.30 (3H, s, CH_3), 2.35 (1H, d, J = 9.4, H-1′), 5.44–5.45 (1H, m, H-3′), 6.06 (1H, dd, J = 9.4; 16.0, ethene), 6.49 (1H, d, J = 16.0, ethene), 6.51 (1H, d, J = 2.4, H-4), 7.16 (1H, d, J = 8.0, Ar), 7.33 (1H, dd, J = 2.2, 8.0, Ar), 7.47 (1H, d, J = 2.2, Ar), 7.77 (1H, d, J = 2.4, H-5). Anal. calcd. for $C_{22}H_{28}N_2$: C, 82.45; H, 8.81; N, 8.74; found: C, 82.39; H, 8.77; N, 8.71.

*5.1.2.7. 2-{5-[2-(2,6,6-trimethylcyclohex-2-enyl)vinyl]pyrazol-1-yl} pyridine (**4g**), 2-{3-[2-(2,6,6-trimethylcyclohex-2-enyl)vinyl]pyrazol-1-yl}pyridine (**5g**).* From 2-hydrazinopyridine dihydrochloride at 50 °C for 1 h (method 1 – see ref. [21]).

*5.1.2.8. (E)-2-(5-(1-(2,6,6-trimethylcyclohex-2-enyl)prop-1-en-2-yl)-1H-pyrazol-1-yl)pyridine (**4h**).* From **3** (1.77 mmol) and phenylydrazine hydrochloride (1.77 mmol) at room temperature for 1 h (method 1). After evaporation to dryness, the residue was chromatographed on silica gel eluting with toluene. The second eluate gave **4h** as a thick yellow oil. Yield 60%. IR (film): ν 2960, 2916, 1591, 1579, 1473, 1436 cm^{-1}; ^1H NMR (200 MHz, $CDCl_3$): δ 0.81 (3H, s, CH_3), 0.92 (3H, s, CH_3), 1.15–1.20 (1H, m, H-5′), 1.35–1.41 (1H, m, H-5′), 1.62 (3H, s, CH_3), 1.87 (3H, s, CH_3), 1.94–1.96 (2H, m, H-4′), 2.54 (1H, d,, H-1′ J = 10.3 Hz), 5.34–5.36 (2H, m, H-4′, ethene), 6.22 (1H, d, H-4, J = 1.4 Hz), 7.15–7.20 (1H, m, Ar), 7.59 (1H, d, H-3, J = 1.4 Hz), 7.65–7.81 (2H, m, Ar), 8.35–8.40 (1H, m, Ar) Anal. calcd. for $C_{20}H_{25}N_3$: C, 78.14; H, 8.20; N, 13.67; found: C, 77.11; H, 8.52; N, 13.84.

*5.1.2.9. 2-{5-[2-(phenyl)vinyl]pyrazol-1-yl}pyridine (**8a**); 2-{3-[2-(phenyl)vinyl]pyrazol-1-yl}pyridine (**9a**).* From 2-hydrazinopyridine dihydrochloride and **7** at 50 °C for 1 h (method 1). The residue was chromatographed on silica gel eluting with CH_2Cl_2/toluene 1:1, toluene. The first eluate gave **9a** as a white solid which was

crystallized from diethyl ether; mp 77–81 °C. Yield 11%. The second eluate gave **8a** as white solid, crystallized from diethyl ether; mp 80–81 °C. Yield 48%. Data of **8a**: IR (KBr): ν 1590, 1471, 1446, 1382, 783 cm^{-1}; ^1H NMR (200 MHz, $CDCl_3$): δ 6.71 (1H, d, J = 1.8, H-4), 7.12 (1H, d, J = 16.4, ethene), 7.22–7.39 (4H, m, Ar), 7.47–7.53 (2H, m, Ar), 7.65–7.68 (1H, m, Ar), 7.85 (1H, d, J = 1.8, H-3), 8.83–7.88 (1H, m, Ar), 7.94 (1H, d, J = 16.4, ethene), 8.46–8.54 (1H, m, Ar). Anal. calcd. for $C_{16}H_{13}N_3$: C, 77.71; H, 5.30; N, 16.99; found: C, 77.65; H, 5.63; N, 17.21. Data of **9a**: IR (KBr): ν 1593, 1472, 1452, 770 cm^{-1}; ^1H NMR (200 MHz, $CDCl_3$): δ 6.69 (1H, d, J = 2.8, H-4), 7.13–7.37 (5H, m, Ar + ethene), 7.33 (1H, d, J = 2.8, H-5); 7.49–7.53 (2H, m, Ar + ethene), 7.80–7.97 (2H, m, Ar), 8.36–8.41 (1H, m, Ar), 8.53–8.55 (1H, m, Ar). Anal. calcd. for $C_{16}H_{13}N_3$: C, 77.71; H, 5.30; N, 16.99; found: C, 77.61; H, 5.38; N, 16.81.

*5.1.2.10. 2-{5-[2-(furan-2-yl)vinyl]-1H-pyrazol-1-yl}pyridine (**8b**); 2-{3-[2-(furan-2-yl)vinyl]-1H-pyrazol-1-yl}pyridine (**9b**).* From 2-hydrazinopyridine dihydrochloride and **7** at 60 °C for 1 h (method 1). The residue was chromatographed on silica gel eluting firstly with CH_2Cl_2/toluene 1:1 and, secondly, with toluene. The first eluate gave **9b** as a red solid which was crystallized from diethyl ether, mp 75–78 °C. Yield 8%. The second eluate gave **8b** as red solid, crystallized from diethyl ether, mp 50–53 °C. Yield 44%. Data of **8b**: IR (KBr): ν 1587, 1472, 1437, 1373 cm^{-1}; ^1H NMR (200 MHz, $CDCl_3$): δ 6.39–6.42 (2H, m, Ar), 6.64 (1H, d, H-4, J = 2.0 Hz), 6.87 (1H, d, J = 16.2, ethene), 7.23–7.27 (1H, m, Ar), 7.39–7.40 (1H, m, Ar), 7.69 (1H, d, J = 16.2, ethene), 7.82 (1H, d, J = 2.0, H-3), 7.82–7.85 (2H, m, Ar), 8.52–8.55 (1H, m, Ar). Anal. calcd. for $C_{14}H_{11}N_3O$: C, 77.71; H, 5.30; N, 16.99; found: C, 77.65; H, 5.42; N, 17.05. Data of **9b**: IR (KBr): ν 1588, 1472, 1439, 1370 cm^{-1}; ^1H NMR (200 MHz, $CDCl_3$): d 6.58–6.61 (2H, m, Ar), 6.78 (1H, d, H-4, J = 2.6 Hz), 7.16 (1H, d, ethene, J = 16.4 Hz), 7.25–7.43 (2H, m, Ar + ethene), 7.59–7.62 (1H, m, Ar), 7.93–8.01 (1H, m, Ar), 8.13–8.17 (1H, m, Ar), 8.56–8.58 (1H, m, Ar), 8.68 (1H, d,H-5, J = 2.6 Hz). Anal. Calcd. for $C_{14}H_{11}N_3O$: C, 77.71; H, 5.30; N, 16.99; found: C, 77.68; H, 5.34; N, 17.04.

*5.1.2.11. 2-{5-[2-(4-chlorophenyl)vinyl]pyrazol-1-yl}pyridine (**8c**); 2-{3-[2-(4-chlorophenyl)vinyl]pyrazol-1-yl}pyridine (**9c**).* From 2-hydrazinopyridine dihydrochloride and **7** at 60 °C for 1 h (method 1). The residue was chromatographed on silica gel eluting with CH_2Cl_2/toluene 1:1 and then toluene. The first eluate gave **9c** as a white solid which was crystallized from diethyl ether, mp 118–121 °C. Yield 8%. The second eluate gave **8c** as yellow solid, crystallized from diethyl ether, mp 64–66 °C. Yield 40%. Data of **8c**: IR (KBr): ν 1590, 1475, 1432, 1378 cm^{-1}; ^1H NMR (200 MHz, $CDCl_3$): δ 6.70 (1H, d, J = 2.0, H-4), 7.03 (1H, d, J = 16,2, ethene), 7.23–7.44 (5H, m, H-4′ and ethene), 7.67 (1H, d, J = 2.0, H-3), 7.84–7.88 (2H, m, Ar), 8.51–8.53 (1H, m, Ar). Anal. Calcd. for $C_{16}H_{12}ClN_3$: C, 68.21; H, 4.29; Cl, 12.58; N, 14.91; found: C, 68.16; H, 4.36; N, 14.94. Data of **9c**: IR (KBr): ν 1595, 1471, 1447, 1377, 774 cm^{-1}; ^1H NMR (200 MHz, $CDCl_3$): δ 6.67 (1H, d, J = 2.6, H-4), 7.09–7.47 (7H, m, Ar + ethane + H-5), 7.82–8.00 (2H, m, Ar), 8.35–8.56 (2H, m, Ar). Anal. calcd. for $C_{16}H_{12}ClN_3$: C, 68.21; H, 4.29; Cl, 12.58; N, 14.91; found: C, 68.18; H, 4.33; N, 14.97.

*5.1.2.12. 2-{5-[2-(3-chlorophenyl)vinyl]pyrazol-1-yl}pyridine (**8d**); 2-{3-[2-(3-chlorophenyl)vinyl]pyrazol-1-yl}pyridine (**9d**).* From 2-hydrazinopyridine dihydrochloride and **7** at 60 °C for 1 h (method 1). The residue was chromatographed on silica gel eluting with CH_2Cl_2/toluene 1:1 and then toluene. The first eluate gave **9d** as a white solid, crystallized from diethyl ether, mp 128–130 °C. Yield 10%. The second eluate gave **8d** as yellow solid, crystallized from cyclohexane, mp 68–70 °C. Yield 44%. Data of **8d**: IR (KBr): ν 1592, 1473, 1435, 1379 cm^{-1}; ^1H NMR (200 MHz, $CDCl_3$): δ 6.70 (1H, d, J = 2.0, H-4), 7.02 (1H, d, J = 16,4, ethene), 7.24–7.37 (4H, m, Ar), 7.47 (1H, s, Ar), 7.67 (1H, d, J = 2.0, H-3), 7.85–7.88 (1H, m, Ar), 7.95 (1H, d, J = 16,4, ethene), 8.53 (1H, m, Ar); ^{13}C NMR (50 MHz, $CDCl_3$): δ 104.8 (CH); 116.0 (CH); 118.3 (CH); 120.8 (CH); 124.0 (CH); 125.5 (CH); 126.9 (2CH); 128.9 (2CH); 133.6 (C); 137.6 (C); 137.8 (CH); 140.0 (CH); 141.0 (C); 146.8 (C). Anal. Calcd. for $C_{16}H_{12}ClN_3$: C, 68.21; H, 4.29; Cl, 12.58; N, 14.91. Found: C, 68.14; H, 4.34; N, 15.17. Data of **9d**: IR (KBr): ν 1594, 1517, 1475, 1449, 1377 cm^{-1}; ^1H NMR (200 MHz, $CDCl_3$): δ 6.68 (1H, d,, H-4 J = 2.6 Hz), 7.15–7.41 (6H, m, Ar + ethene + H-5), 7.50–7.51 (1H, m, Ar), 7.78–7.87 (1H, m, Ar), 7.97–8.01 (1H, m, Ar), 8.40–8.42 (1H, m, Ar), 8.56 (1H, m, Ar); ^{13}C NMR (50 MHz, $CDCl_3$): δ 107.9 (CH); 114.8 (CH); 123.9 (CH); 124.4 (CH); 127.3 (CH); 129.1 (2CH); 130.3 (2CH); 130.7(CH), 132.50 (C); 137.2 (C); 141.3 (CH); 150.6 (C); 153.2 (C). Anal. Calcd. for $C_{16}H_{12}ClN_3$: C, 68.21; H, 4.29; Cl, 12.58; N, 14.91; found: C, 68.13; H, 4.26; N, 14.74.

*5.1.2.13. 2-{5-[2-(3,4-dimethoxyphenyl)vinyl]pyrazol-1-yl}pyridine (**8e**).* From 2-hydrazinopyridine dihydrochloride and **7** at 60 °C for 1 h (method 1). After cooling, the solid was collected by filtration from the mixture and crystallized from ethanol, mp 126–128 °C. Yield 73%. IR (KBr): ν 1591, 1512, 1470, 1438, 1379 cm^{-1}; ^1H NMR (200 MHz, $CDCl_3$): δ 3.90 (3H, s, OCH_3), 3.92 (3H, s, OCH_3), 6.68 (1H, d, H-4, J = 2.0 Hz), 6.85 (1H, d, Ar), 7.06 (1H, d J = 16,4, ethene), 7.03–7.04 (2H, m, Ar), 7.25 (1H, s, Ar), 7.68 (1H, d, J = 2.0, H-3), 7.73 (1H, d, J = 16,4, ethene), 7.85–7.89 (2H, m, Ar), 8.48–8.53 (1H, m, Ar). Anal. calcd. for $C_{18}H_{17}N_3O_2$: C, 70.34; H, 5.58; N, 13.67; found: C, 70.42; H, 5.85; N, 13.48.

*5.1.3. General procedure for the synthesis of compounds **11***

A suspension or a solution of each methylketone (10 mmol) in xylene (30 mmol) was treated with dimethylformamide dimethylacetal (10 mmol). The reaction mixture was refluxed for different hours. After cooling, compound **11a**, **11e**, **11g**, **11i** and **11l** were obtained by silica gel chromatography of the residue after removal of the solvent. All the other compounds were collected by filtration from the mixture and crystallized.

*5.1.3.1. (2E)-3-(dimethylamino)-1-(4-methoxyphenyl)-2-propen-1-one (**11a**).* From 4′-methoxyacetophenone, refluxed for 2 h. The residue was chromatographed on silica gel eluting with toluene/AcOEt 1:1 and, then, AcOEt. The first eluate gave the starting product, the second eluate gave **11a** as a yellow solid, mp 89–91 °C. Yield 62%. IR (KBr): ν1638, 1580, 1539, 1359, 1241 cm^{-1}; ^1H NMR (200 MHz, $CDCl_3$): δ 3.03 (6H, s, NCH_3), 3.86 (3H, s, OCH_3), 5.73 (1H, d, J = 12.6, CH-2), 6.92 (2H, d, J = 8.5, Ar), 7.45 (1H, d, J = 12.6, CH-3), 7.92 (2H, d, J = 8.5, Ar); Anal. calcd. for $C_{12}H_{15}NO_2$: C, 70.22; H, 7.37; N, 6.82; found: C, 70.26; H, 7.30; N, 6.74.

*5.1.3.2. (2E)-3-(dimethylamino)-1-(2-hydroxy-5-methylphenyl)-2-propen-1-one (**11b**).* From 2′-hydroxy-5′-methylacetophenone, refluxed for 2 h. An orange solid was collected by filtration from the mixture and crystallized from EtOH, mp 136–138 °C. Yield 65%. IR (KBr): ν 1634, 1532, 1498, 1341, 1291 cm^{-1}; ^1H NMR (200 MHz, $CDCl_3$): δ 2.33 (3H, s, CH_3), 3.01 (3H, s, NCH_3), 3.21 (3H, s, NCH_3), 5.80 (1H, d, J = 12.0, CH-2), 6.87 (2H, d, J = 8.2, CH-2), 7.20 (2H, dd, J = 8.2, 1.6, CH-2), 7.50 (2H, d, J = 8.5, Ar), 7.90 (1H, d,, J = 12.0, CH-3). Anal. calcd. for $C_{12}H_{15}NO_2$: C, 70.22; H, 7.37; N, 6.82; found: C, 70.44; H, 7.71; N, 6.75.

*5.1.3.3. (2E)-1-(5-chloro-2-hydroxyphenyl)-3-(dimethylamino)-2-propen-1-one (**11c**).* From 5′-chloro-2′-hydroxyacetophenone, refluxed for 2 h. A yellow solid was collected by filtration from the mixture and crystallized from cyclohexane, mp 141 °C. Yield 70%. IR (KBr): ν 1633, 1540, 1477, 1286 cm^{-1}; ^1H NMR (200 MHz, $CDCl_3$):

δ 3.02 (3H, s, NCH_3), 3.24 (3H, s, NCH_3), 5.70 (1H, d, $J = 12.1$, CH-2), 6.90 (2H, d, $J = 8.8$, Ar), 7.31 (2H, dd, $J = 8.8$, 2.6 Ar), 7.65 (2H, d, $J = 8.8$ Ar), 7.92 (1H, d, $J = 12.1$, CH-3). Anal. calcd. for $C_{11}H_{12}ClNO_2$: C, 58.54; H, 5.36; N, 6.21; found: C, 58.74; H, 5.71; N, 6.21.

*5.1.3.4. (2E)-3-(dimethylamino)-1-(2-hydroxy-4-methoxyphenyl)-2-propen-1-one (**11d**).* From 2′-hydroxy-4′-methoxyacetophenone, refluxed for 2 h. A yellow solid was collected by filtration from the mixture and crystallized from EtOH, mp 145–146 °C. Yield 56%. IR (KBr): ν 1625, 1543, 1443, 1369, 1237 cm^{-1}; ^1H NMR (200 MHz, $CDCl_3$): δ 2.97 (3H, s, NCH_3), 3.17 (3H, s, NCH_3), 3.83 (3H, s, OCH_3), 5.71 (1H, d, $J = 12.6$, CH-2), 6.37–6.43 (2H, m, Ar), 7.61 (2H, d, $J = 8.9$, Ar), 7.88 (1H, d, $J = 12.6$, CH-3). Anal. calcd. for $C_{12}H_{15}NO_3$: C, 65.14; H, 6.83; N, 6.33; found: C, 65.20; H, 7.05; N, 6.59.

*5.1.3.5. N-[4-[(2E)-3-(dimethylamino)-1-oxo-2-propen-1-yl]phenyl]-acetamide (**11e**).* From N-(4-acetylphenyl)-acetamide, refluxed for 2 h. The residue was chromatographed on silica gel eluting firstly with toluene/AcOEt 1:1 and, secondly, with AcOEt/EtOH. The first eluate gave the starting product, the second eluate gave **11e** as a yellow solid which was crystallized from cyclohexane, mp 183–185 °C. Yield 36%. IR (KBr): ν 1690, 1638, 1552, 1262 cm^{-1}; ^1H NMR (200 MHz, $CDCl_3$): δ 2.07 (3H, s, $C(O)CH_3$), 2.97 (6H, s, NCH_3), 5.73 (1H, d, $J = 12.6$, CH-2), 7.62 (2H, d, $J = 8.6$, Ar), 7.78 (1H, d, $J = 12.6$, CH-3), 7.86 (2H, d, $J = 8.6$, Ar), 8.91 (1H, s, NH). Anal. ($C_{13}H_{16}N_2O_2$) C, H, N. Anal. calcd. for $C_{13}H_{16}N_2O_2$: C, 67.22; H, 6.94; N, 12.06; found: C, 67.40; H, 7.20; N, 11.93.

*5.1.3.6. (2E)-3-(dimethylamino)-1-(2-hydroxyphenyl)-2-propen-1-one (**11f**).* From 2′-hydroxyacetophenone, refluxed for 2 h. A yellow solid was collected by filtration from the mixture and crystallized from EtOH, mp 130–132 °C. Yield 82%. IR (KBr): ν 1629, 1489, 1287 cm^{-1}; ^1H NMR (200 MHz, $CDCl_3$): δ 2.99 (3H, s, NCH_3), 3.21 (3H, s, NCH_3), 5.80 (1H, d, $J = 12.2$, CH-2), 6.80–6.98 (2H, m, Ar), 7.34–7.41 (1H, m, Ar), 7.70–7.75 (1H, m, Ar), 7.61 (2H, d, $J = 8.9$, Ar), 7.91 (1H, d, $J = 12.2$, CH-3), 13.97 (1H, s, OH). Anal. calcd. for $C_{11}H_{13}NO_2$: C, 69.09; H, 6.85; N, 7.32; found: C, 69.18; H, 6.51; N, 7.45.

*5.1.3.7. (2E)-3-(dimethylamino)-1-(3-methoxyphenyl)-2-propen-1-one (**11g**).* From 3′-methoxyacetophenone, refluxed for 2 h. The residue was chromatographed on silica gel eluting with toluene/AcOEt 8:2 and, then, with AcOEt. The first eluate gave the starting product, the second eluate gave **11g** as an orange oil. Yield 79%. IR (film): ν 1638, 1560, 1437, 1358, 1261 cm^{-1}; ^1H NMR (200 MHz, $CDCl_3$): δ 2.96 (3H, s, NCH_3), 3.13 (3H, s, NCH_3), 3.87 (3H, s, OCH_3), 5.71 (1H, d, $J = 12.4$, CH-2), 6.99–7.05 (1H, m, Ar), 7.29–7.37 (1H, m, Ar), 7.45–7.49 (2H, m, Ar), 7.83 (1H, d, $J = 12.4$, CH-3). Anal. calcd. for $C_{15}H_{16}N_2O_2$: C, 70.22; H, 7.37; N, 6.82; found: C, 70.22; H, 7.58; N, 6.97.

*5.1.3.8. (2E)-3-(dimethylamino)-1-(4-morpholinophenyl)-2-propen-1-one (**11h**).* From 4′-morpholinoacetophenone, refluxed overnight. A white solid was collected by filtration from the mixture and crystallized from AcOEt, mp 205–207 °C. Yield 33%. IR (KBr): ν 1634, 1599, 1571, 1528 cm^{-1}; ^1H NMR (200 MHz, $CDCl_3$): δ 3.04 (6H, s, NCH_3), 3.28 (4H, *t*, NCH_2), 3.89 (4H, *t*, O CH_2), 5.75 (1H, d, $J = 12.4$, CH-2), 6.91 (2H, d, $J = 9.0$, Ar), 7.81 (1H, d, $J = 12.4$, CH-3), 7.92 (2H, d, $J = 8.9$, Ar). Anal. calcd. for $C_{15}H_{20}N_2O_2$: C, 69.20; H, 7.74; N, 10.76; found: C, 69.21; H, 7.97; N, 10.43.

*5.1.3.9. (2E)-3-(dimethylamino)-1-(2,4-dimethoxyphenyl)-2-propen-1-one (**11i**).* From 2′, 4′-dimethoxyacetophenone, refluxed for 2 days. The residue was chromatographed on silica gel eluting with toluene/AcOEt 9:1 and, then, AcOEt. The first eluate gave the starting product, the second eluate gave **11i** as a dark yellow oil. Yield 32%. IR (KBr): ν 1631, 1541, 1442, 1368, 1237 cm^{-1}; ^1H NMR (200 MHz, $CDCl_3$): δ 2.97 (3H, s, NCH_3), 3.15 (3H, s, NCH_3), 3.72 (3H, s, OCH_3), 3.83 (3H, s, OCH_3), 5.74 (1H, d, $J = 12.6$, CH-2), 6.57–6.68 (2H, m, Ar), 7.61 (2H, d, $J = 8.9$, Ar), 7.78 (1H, d, $J = 12.6$, CH-3), 7.83–7.85 (1H, m, Ar). Anal. calcd. for $C_{15}H_{17}NO_3$: C, 66.36; H, 7.28; N, 5.95; found: C, 66.30; H, 7.25; N, 6.01.

*5.1.3.10. (2E)-3-(dimethylamino)-1-(2-methoxyphenyl)-2-propen-1-one (**11l**).* From 2′ methoxyacetophenone, refluxed overnight. The residue was chromatographed on silica gel eluting with toluene/AcOEt 9:1 and, then, AcOEt. The first eluate gave the starting product, the second eluate gave **11l** as a yellow oil. Yield 44%. IR (KBr): ν 1631, 1538, 1447, 1362, 1237 cm^{-1}; ^1H NMR (200 MHz, $CDCl_3$): δ 3.05 (6H, s, NCH_3), 3.78 (3H, s, OCH_3), 5.76 (1H, d, $J = 12.6$, CH-2), 7.02–7.08 (1H, m, Ar), 7.40–7.56 (2H, m, Ar), 7.68 (1H, d, $J = 12.6$, CH-3), 7.78–7.85 (1H, m, Ar); Anal. calcd. for $C_{12}H_{15}NO_2$: C, 70.22; H, 7.37; N, 6.82; found: C, 70.25; H, 7.32; N, 6.76.

*5.1.4. General procedure for the synthesis of compounds **12** and **13***

The hydrazines (method 2) or hydrazine hydrochlorides (method 1) (2 mmol) were added in one portion to a stirred solution of the appropriate compound **11** (2 mmol) in acidified EtOH [10 mL containing 0.17 mL of HCl 37% (method 2)] or EtOH [10 mL (method 1)]. The resulting solution was stirred for 2 h at 60 °C.

*5.1.4.1. 2-[5-(4-methoxyphenyl)-1H-pyrazol-1-yl]pyridine (**12a**); 2-[3-(4-methoxyphenyl)-1H-pyrazol-1-yl]pyridine (**13a**).* From 2-hydrazinopyridine dihydrochloride and **11a** (method 1). The residue was chromatographed on silica gel eluting with toluene and, then, toluene/AcOEt 1:1. The first eluate gave **13a** as a pale yellow solid which was crystallized from diethyl ether, mp 75–77 °C. Yield 6%. The second eluate gave **12a** as yellow oil. Yield 43%. Data of **12a**: IR (film): ν 2936, 2836, 1591, 1499, 1473, 1458, 1378 cm^{-1}; ^1H NMR (200 MHz, $CDCl_3$): δ3.96 (3H, s, OCH_3), 6.09 (1H, d, $J = 1.8$, H-4), 6.98–7.02 (2H, m, Ar), 7.32–7.39 (3H, m, Ar), 7.55–7.61 (1H, m, Ar), 7.83–7.96 (1H, m, Ar), 7.90 (1H, d, $J = 1.8$, H-3), 8.54–8.61 (1H, m, Ar); ^{13}C NMR (50 MHz, $CDCl_3$): δ 54.2 (OCH_3), 107.3 (CH), 112.7 (2CH), 118.0 (CH), 121.4 (CH), 122.3 (C), 129.0 (2CH), 137.1 (CH), 140.0 (CH), 142.4 (C), 147.5 (CH), 151.5 (C), 158.5 (C). Anal. calcd. for $C_{15}H_{13}N_3O$: C, 71.70; H, 5.21; N, 16.72. Found: C, 71.63; H, 5.13; N, 16.48. Data of **13a**: IR (film): ν 2936, 2836, 1591, 1499, 1473, 1458, 1378 cm^{-1}; ^1H NMR (200 MHz, $CDCl_3$): δ 4.03 (3H, s, OCH_3), 6.89 (1H, d, $J = 2.6$, H-4), 7.14 (2H, d, Ar), 7.30–7.39 (1H, m, Ar), 7.55–7.61 (1H, m, Ar), 7.98–8.05 (3H, m, Ar), 8.25–8.30 (1H, m, Ar), 8.54–8.61 (1H, m, Ar); 8.76 (1H, d, $J = 2.6$, H-5). Anal. calcd. for $C_{15}H_{13}N_3O$: C, 71.70; H, 5.21; N, 16.72; found: C, 71.68; H, 5.19; N, 16.89.

*5.1.4.2. 1-(4-chlorophenyl)-5-(4-methoxyphenyl)-1H-pyrazole (**12a1**); 1-(4-chlorophenyl)-3-(4-methoxyphenyl)-1H-pyrazole (**13a1**).* From 4-chlorophenylhydrazine hydrochloride and **11a** (method 1). The residue was chromatographed on silica gel eluting with dichloromethane. The first eluate gave **13a1** as a pale yellow solid which was crystallized from diethyl ether, mp 75–77 °C. Yield 6%. The second eluate gave **12a1** as a red oil. Yield 53%. Data of **12a1:** IR (film): ν 2836, 1613, 1497, 1452, 1383, 1251 cm^{-1}; ^1H NMR (200 MHz, $CDCl_3$): δ 3.98 (3H, s, OCH_3), 6.11 (1H, d, $J = 1.8$, H-4), 6.99–7.04 (2H, m, Ar), 7.29–7.50 (6H, m, Ar), 7.86 (1H, d, $J = 1.8$, H-3); ^{13}C NMR (50 MHz, $CDCl_3$): δ 54.2 (OCH_3), 106.7 (CH), 113.0 (2CH), 121.6 (C), 125.2 (2CH), 128.0 (2CH), 129.0 (2CH), 131.9 (C), 137.7 (C), 139.5 (CH), 141.9 (C), 158.6 (C). Anal. calcd. for $C_{16}H_{13}ClN_2O$: C, 67.49; H, 4.60; Cl, 12.45; N, 9.84; found: C, 67.30; H, 4.90; N, 10.07. Data of **13a1**: ^1H NMR (200 MHz, $CDCl_3$): δ 4.02 (3H, s, OCH_3), 6.88 (1H, d, $J = 2.6$, H-4), 7.13 (2H, d, Ar), 7.59 (2H, d, Ar), 7.87 (2H, d, Ar), 8.00

(2H, d, Ar), 8.06 (1H, d, $J = 2.6$, H-5). Anal. calcd. for $C_{16}H_{13}ClN_2O$: C, 67.49; H, 4.60; Cl, 12.45; N, 9.84; found: C, 67.39; H, 4.67; N, 10.02.

*5.1.4.3. 2-[1-(4-chlorophenyl)-1H-pyrazol-5-yl]-4-methylphenol (**12b1**).* From 4-chlorophenylhydrazine hydrochloride and **11b** (method 1). The residue was prified on silica gel eluting with toluene/AcOEt 9:1. The eluate gave a white solid which was crystallized from cyclohexane, mp 158–160 °C. Yield 46%. IR (KBr): ν 3154, 1494, 1411, 1270 cm^{-1}; ^1H NMR (200 MHz, $CDCl_3$): δ 2.38 (3H, s, CH_3), 5.30 (1H, s, OH, D_2O exchangeable), 6.69 (1H, d, $J = 1.8$, H-4), 6.94–7.01 (2H, m, Ar), 7.20–7.29 (1H, m, Ar), 7.42(4H, m, Ar), 7.94 (1H, d, $J = 1.8$, H-3); ^{13}C NMR (50 MHz, $CDCl_3$): δ 19.3 (CH_3), 108.0 (CH), 115.0 (CH), 115.7 (C), 124.0 (2CH), 127.9 (2CH), 129.0 (C), 130.0 (CH), 130.4 (CH), 131.8 (C), 137.2 (C), 137.5 (C), 139.7 (CH), 150.0 (C). Anal. calcd. for $C_{16}H_{13}ClN_2O$: C, 67.49; H, 4.60; Cl, 12.45; N, 9.84; found: C, 67.46; H, 4.56; N, 9.73.

*5.1.4.4. 4-Chloro-2-[1-(pyridin-2-yl)-1H-pyrazol-5-yl]phenol (**12c**); 4-chloro-2-[1-(pyridin-2-yl)-1H-pyrazol-3-yl]phenol (**13c**); 6-chloro-4H-chromen-4-one (**14c**).* From 2-hydrazinopyridine dihydrochloride and **11c** (method 1). The residue was chromatographed on silica gel eluting with hexane/AcOEt 8:2. The first eluate gave **13c** as a white solid which was crystallized from diethyl ether, mp 189–190 °C. Yield 14%. The second eluate gave **14c** as a white solid. The third eluate gave **12c** as white solid, crystallized from diethyl ether, mp 40–42 °C. Yield 38%. Data of **12c**: IR (KBr): ν 3067, 1591, 1478, 1437 cm^{-1}; ^1H NMR (200 MHz, $CDCl_3$): δ 6.59 (1H, d, $J = 1.8$, H-4), 7.21 (1H, d, Ar), 7.30 (1H, m, Ar), 7.43–7.53 (2H, m, Ar), 7.96 (1H, d, Ar), 8.08 (1H, d, H-3, $J = 1.8$, H-3), 7.98–8.03 (1H, m, Ar), 8.48–8.50 (1H, m, Ar), 8.83 (1H, m, Ar), 10.58 (1H, s, OH, D_2O exchangeable); ^{13}C NMR (50 MHz, $CDCl_3$): δ 111.9 (CH), 118.6 (CH), 121.2 (C), 122.3 (C), 122.5 (CH), 125.0 (C), 130.4 (CH), 131.5 (CH), 139.7 (C), 140.0 (CH), 141.5 (CH), 145.9 (CH), 151.6 (C), 154.0 (C). Anal. calcd. for $C_{14}H_{10}N_3ClO$: C, 61.89; H, 3.71; Cl, 13.05; N, 15.47; found: C, 61.87; H, 4.00; Cl, N, 15.59. GS-MS $t_r = 20.4$ min, m/z : 271 (M^+). Data of **13c**: IR (KBr): ν 3121, 1581, 1471, 1452 cm^{-1}; ^1H NMR (200 MHz, $CDCl_3$): δ 7.00 (1H, d, $J = 2.6$, H-4), 7.17 (1H, d, Ar), 7.35–7.44 (3H, m, Ar), 7.75 (1H, d, $J = 2.6$, H-5), 8.01–8.04 (2H, m, Ar), 8.60–8.63 (1H, m, Ar), 8.82–8.83 (1H, m, Ar), 10.85 (1H, s, OH, D_2O exchangeable); ^{13}C NMR (50 MHz, $CDCl_3$): δ 104.6 (CH), 111.5 (CH), 117.0 (C), 118.2 (CH), 121.5 (CH), 123.8 (C), 126.0 (CH), 127.9 (CH), 129.3 (CH), 138.6 (CH), 148.0 (CH), 150.0 (C), 152.2 (C), 154.3 (C). Anal. calcd. for $C_{14}H_{10}N_3ClO$: C, 61.89; H, 3.71; Cl, 13.05; N, 15.47; found: C, 61.85; H, 3.83; N, 15.65. GS-MS $t_r = 22.8$ min, m/z : 271 (M^+). Data of **14c**: GS-MS $t_r = 14.3$ min, m/z : 180 (M^+).

*5.1.4.5. 4-Chloro-2-[1-(4-chlorophenyl)-1H-pyrazol-5-yl]phenol (**12c1**).* From 4-chlorophenylhydrazine hydrochloride and **11c** (method *1*). A yellow solid was collected by filtration from the mixture and crystallized from cyclohexane, mp 181–183 °C. Yield 63%. IR (KBr): ν 3099, 1493, 1406, 1276 cm^{-1}; ^1H NMR (200 MHz, (D_6)DMSO): δ 6.71 (1H, d, H-4 $J = 1.8$ Hz), 6.96 (1H, m, Ar), 7.41–7.63 (6H, m, Ar), 7.91 (1H, d, H-3, $J = 1.8$ Hz), 10.08 (1H, s, OH, D_2O exchangeable); ^{13}C NMR (50 MHz, $CDCl_3$): δ 108.3 (CH), 118.9 (CH), 119.1 (C), 124.0 (2CH), 128.0 (2CH), 128.7 (C), 129.3 (CH), 129.5 (CH), 132.0 (C), 136.5 (C), 137.4 (C), 139.6 (CH), 154.6 (C). Anal. calcd. for $C_{15}H_{10}N_2Cl_2O$: C, 59.04; H, 3.30; Cl, 23.24; N, 9.18; found: C, 58.78; H, 3.52; N, 9.01.

*5.1.4.6. 5-Methoxy-2-[1-(pyridin-2-yl)-1H-pyrazol-5-yl]phenol (**12d**); 5-methoxy-2-[1-(pyridin-2-yl)-1H-pyrazol-3-yl]phenol (**13d**); 7-methoxy-4H-chromen-4-one (**14d**).* From 2-hydrazinopyridine dihydrochloride and **11d** (method 1). The residue was chromatographed on silica gel eluting with hexane/AcOEt 8:2. The first eluate gave **13d** as a white solid, crystallized from diethyl ether, mp 87–88 °C. Yield 27%. The second eluate gave **14d** as a white solid. The third eluate gave **12d** as white solid, crystallized from diethyl ether, mp 95–97 °C. Yield 48%. Data of **12d**: IR (KBr): ν 3009, 1618, 1601,1574, 1477, 1292, 1164 cm^{-1}; ^1H NMR (200 MHz, $CDCl_3$): δ 3.97 (3H, s, OCH_3), 6.55 (1H, d, $J = 1.6$, H-4), 6.67 (1H, dd, Ar), 6.85 (1H, d, Ar), 7.22 (1H, d, Ar), 7.43–7.52 (1H, m, Ar), 7.91–7.95 (2H, m, Ar + H-3), 8.04–8.09 (1H, m, Ar), 8.44–8.48 (1H, m, Ar); ^{13}C NMR (50 MHz, $CDCl_3$): δ 54.3 (OCH_3), 104.0 (CH), 106.2 (CH), 110.9 (CH), 112.3 (C), 118.1 (CH), 121.6 (CH), 132.2 (CH), 139.0 (CH), 140.4 (C), 140.7 (CH), 145.2 (CH), 151.2 (C), 155.8 (C), 161.1 (C). Anal. calcd. for $C_{15}H_{13}N_3O_2$: C, 67.40; H, 4.90; N, 15.51; found: C, 67.28; H, 5.06; N, 15.51. GS-MS $t_r = 21.2$ min, m/z : 267 (M^+). Data of **13d**: IR (KBr): ν 1634, 1587, 1438, 1254, 1032 cm^{-1}; ^1H NMR (200 MHz, $CDCl_3$): δ 4.01 (3H, s, OCH_3), 6.65–6.79 (2H, m, Ar), 6.94 (1H, d, $J = 2.8$, H-4), 7.32–7.43 (1H, m, Ar), 7.67–7.72 (1H, m, Ar), 8.00–8.03 (2H, m, Ar + H-5), 8.58–8.62 (1H, m, Ar), 8.77–8.79 (1H, m, Ar), 10.95 (1H, s, OH, D_2O exchangeable); ^{13}C NMR (50 MHz, $CDCl_3$): δ 54.3 (OCH_3), 100.6 (CH), 103.3 (CH), 105.6 (CH), 108.3 (C), 110.7 (CH), 120.4 (CH), 126.8 (CH), 126.9 (CH), 137.8 (CH), 147.2 (CH), 149.5 (C), 152.8 (C), 156.5 (C), 160.2 (C). Anal. calcd. for $C_{15}H_{13}N_3O_2$: C, 67.40; H, 4.90; N, 15.51; found: C, 67.30; H, 4.86; N, 15.72. GS-MS $t_r = 23.4$ min, m/z : 267 (M^+). Data of **14d**: GS-MS $t_r = 15.4$ min, m/z : 176 (M^+).

*5.1.4.7. 2-[1-(4-chlorophenyl)-1H-pyrazol-5-yl]-5-methoxyphenol (**12d1**).* From 4-chlorophenylhydrazine hydrochloride and **11d** (method 1). A yellow solid was collected by filtration from the mixture and crystallized from diethyl ether, mp 147–148 °C. Yield 66%. IR (KBr): ν 3135, 1496, 1208, 829 cm^{-1}; ^1H NMR (200 MHz, $CDCl_3$): δ 3.94 (3H, s, OCH_3), 6.01 (1H, s, OH, D_2O exchangeable), 6.59–6.63 (2H, m, Ar), 6.66 (1H, d, $J = 1.8$, H-4), 7.01–7.10 (1H, m, Ar), 7.39–7.43 (4H, m, Ar), 7.91 (1H, d, $J = 1.8$, H-3); ^{13}C NMR (50 MHz, $CDCl_3$): δ 54.6 (OCH_3), 101.0 (CH), 104.6 (CH), 108.6 (CH), 109.8 (C), 124.3 (2CH), 128.3 (2CH), 130.5 (CH), 131.3 (C), 139.4 (C), 139.5 (C), 139.6 (CH), 155.4 (C), 160.6 (C). Anal. calcd. for $C_{16}H_{13}N_2ClO_2$: C, 63.90; H, 4.36; N, 9.31; found: C, 63.78; H, 4.30; N, 9.38.

*5.1.4.8. N-{4-[(1-(pyridin-2-yl)-1H-pyrazol-5-yl)]phenyl}ethanamide (**12e**).* From 2-hydrazinopyridine dihydrochloride and **11e** (method 1). The residue was chromatographed on silica gel eluting with toluene and, then, toluene/AcOEt 1:1. The eluate gave **12e** as a white solid, crystallized from EtOH, mp 179–181 °C. Yield 23%. IR (KBr): ν 1687, 1595, 1504, 1477, 1436 cm^{-1}; ^1H NMR (200 MHz, $CDCl_3$): δ 2.11 (3H, s, CH_3), 6.64 (1H, d, $J = 1.8$, H-4), 7.25 (2H, d, Ar), 7.43 (1H, s, NH, D_2O exchangeable), 7.77 (1H, m, Ar), 7.90 (1H, d, $J = 1.8$, H-3), 7.97–8.04 (1H, m, Ar), 8.31–8.37 (1H, m, Ar), 8.51–8.58 (1H, m, Ar); ^{13}C NMR (50 MHz, $CDCl_3$): δ 23.3 (CH_3), 104.7 (CH), 112.2 (CH), 118.1 (2CH), 121.8 (CH), 125.0 (C), 128.2 (2CH), 137.3 (C), 137.7 (CH), 140.1 (CH), 141.2 (C), 147.2 (CH), 151.6 (C), 160.7 ($C = O$). Anal. calcd. for $C_{16}H_{14}N_4O$: C, 69.05; H, 5.07; N, 20.13; found: C, 69.18; H, 5.20; N, 20.27.

*5.1.4.9. 2-[1-(pyridin-2-yl)-1H-pyrazol-5-yl]phenol (12f); 2-[1-(pyridin-2-yl)-1H-pyrazol-3-yl]phenol (13f); 4-oxo-chromene (**14f**).* From 2-hydrazinopyridine dihydrochloride and **11f** (method 1). The residue was chromatographed on silica gel eluting with hexane/AcOEt 9:1 and, then, AcOEt. The first eluate gave **13f** as a white solid, crystallized from diethyl ether, mp 96–98 °C. Yield 28%. The second eluate gave **14f** as a white solid. The third eluate gave **12f** as white solid, crystallized from diethyl ether, mp 170–173 °C. Yield 44%. Data of **12f** : IR (KBr): ν 3050, 1478, 1438, 1365 cm^{-1}; ^1H NMR (200 MHz, d_6-DMSO): δ 6.64 (1H, d, $J = 1.8$, H-4), 6.87–7.00 (2H, m, Ar), 7.27–7.42 (2H, m, Ar), 7.27–7.42 (2H, m, Ar), 7.43–7.46 (1H, m, Ar), 7.77–7.84 (1H, m, Ar), 7.90 (1H, m, $J = 1.8$, H-3), 8.04–8.08 (1H, m, Ar), 8.31–8.34 (1H, m, Ar), 9.54 (1H, s, OH, D_2O exchangeable);

^{13}C NMR (50 MHz, $CDCl_3$): δ 111.0 (CH), 117.9 (CH), 119.1 (CH), 119.6 (CH), 120.2 (C), 121.6 (CH), 130.0 (CH), 131.4 (CH), 139.0 (CH), 140.4 (C), 140.7 (CH), 145.3 (CH), 151.1 (C), 154.5 (C). Anal. calcd. for $C_{14}H_{11}N_3O$: C, 70.87; H, 4.67; N, 17.71; found: C, 70.91; H, 4.62; N, 17.71. GS-MS t_r = 18.8 min, *m/z* : 237 (M^+). Data of **13f** : IR (KBr): ν 3142, 1576, 1472, 1445, 1365 cm^{-1}; ^{1}H NMR (200 MHz, $CDCl_3$): δ 7.04 (1H, d,, H-4 *J* = 2.8 Hz), 7.09–7.50 (4H, m, Ar + H-4), 7.79–7.83 (1H, m, Ar), 8.02–8.06 (2H, m, *J* = 2.6, H-5), 8.59–8.63 (1H, m, Ar), 8.14–8.24 (1H, m, Ar), 10.87 (1H, s, OH, D_2O exchangeable); ^{13}C NMR (50 MHz, $CDCl_3$): δ 103.9 (CH), 110.9 (CH), 115.0 (C), 116.1 (CH), 118.5 (CH), 120.6 (CH), 125.9 (CH), 127.0 (CH), 128.9 (CH), 137.9 (CH), 147.2 (CH), 149.4 (C), 152.8 (C), 155.0 (C). Anal. calcd. for $C_{14}H_{11}N_3O$: C, 70.87; H, 4.67; N, 17.71; found: C, 70.82; H, 4.70; N, 17.99. GS-MS t_r = 21.0 min, *m/z* : 237 (M^+). Data of **14f**: GS-MS t_r = 11.5 min, *m/z* : 146 (M^+).

*5.1.4.10. 2-[1-(4-chlorophenyl)-1H-pyrazol-5-yl]phenol (**12f1**).* From 4-chlorophenylhydrazine hydrochloride and **11f** (method 1). A white solid was collected by filtration from the mixture and crystallized from cyclohexane, mp 184–187 °C. Yield 55%. IR (KBr): ν 3428, 2967, 1497, 834, 756 cm^{-1}; ^{1}H NMR (200 MHz, (D_6)DMSO): δ 6.63(1H, d, *J* = 1.8, H-4), 6.96–7.03 (2H, m, Ar), 7.29–7.43 (4H, m, Ar), 7.52–7.58 (2H, m, Ar), 7.89 (1H, d, *J* = 1.8, H-3), 9.80 (1H, s, OH, D_2O exchangeable); ^{13}C NMR (50 MHz, $CDCl_3$): δ 108.7 (CH), 115.4 (CH), 117.1 (C), 118.7 (CH), 124.3 (2CH), 128.3 (2CH), 130.1 (C), 130.7 (CH), 139.3 (C), 139.6 (C), 139.7 (CH), 154.3 (C). Anal. calcd. for $C_{15}H_{11}N_2ClO$: C, 66.55; H, 4.10; N, 10.35; found: C, 66.58; H, 4.16; N, 10.32. GS-MS t_r = 19.9 min, *m/z* : 270 (M^+).

*5.1.4.11. 2-[5-(3-methoxyphenyl)-1H-pyrazol-1-yl]pyridine (12l); 2-[3-(3-methoxyphenyl)-1H-pyrazol-1-yl]pyridine (**13l**).* From 2-hydr-azinopyridine dihydrochloride and **11l** (method 1). The residue was chromatographed on silica gel eluting with toluene and, then, toluene/AcOEt 1:1. The first eluate gave **13l** as a pale yellow oil. Yield 11%. The second eluate gave **12l** as yellow solid, crystallized from diethyl ether, mp 61–63 °C. Yield 50%. Data of **12l**: IR (KBr): ν 2938, 2835, 1590, 1472, 1434, 1378 cm^{-1}; ^{1}H NMR (200 MHz, $CDCl_3$): δ 3.88 (3H, s, OCH_3), 6.69 (1H, d, *J* = 1.8, H-4), 6.97–7.04 (3H, m, Ar), 7.36–7.43 (2H, m, Ar), 7.58–7.64 (1H, m, Ar), 7.85–7.97 (1H, m, Ar), 7.92 (1H, d, *J* = 1.8, H-3), 8.53–8.60 (1H, m, Ar); ^{13}C NMR (50 MHz, $CDCl_3$): δ 54.1 (OCH_3), 107.8 (CH), 112.9 (CH), 113.1 (CH), 118.0 (CH), 120.1 (CH), 121.5 (CH), 128.3 (CH), 131.1 (C), 137.1 (CH), 140.0 (CH), 142.4 (C), 147.5 (CH), 151.4 (C), 158.3 (C). Anal. calcd. for $C_{15}H_{13}N_3O$: C, 71.70; H, 5.21; N, 16.72. found: C, 71.66; H, 5.43; N, 16.67. GS-MS t_r = 19.5 min, *m/z* : 251 (M^+). Data of **13l**: IR (film): ν 2937, 2835, 1595, 1578, 1473, 1454, 1355 cm^{-1}; ^{1}H NMR (200 MHz, $CDCl_3$): δ 4.06 (3H, s, OCH_3), 6.69 (1H, d, *J* = 2.6, H-4), 7.05–7.11 (1H, m, Ar), 7.48–7.56 (1H, m, Ar), 7.58–7.64 (2H, m, Ar), 7.92–8.04 (1H, m, Ar), 8.25–8.30 (1H, m, Ar), 8.57–8.59 (1H, m, Ar), 8.76 (1H, d, *J* = 2.6, H-5); ^{13}C NMR (50 MHz, $CDCl_3$): δ 54.3 (OCH_3), 104.4 (CH), 110.0 (CH), 111.4 (CH), 113.1 (CH), 117.5 (CH), 120.2 (CH), 127.2 (CH), 128.6 (CH), 133.2 (C), 137.6 (CH), 146.9 (CH), 150.2 (C), 152.5 (C), 158.8 (C). Anal. calcd. for $C_{15}H_{13}N_3O$: C, 71.70; H, 5.21; N, 16.72; found: C, 71.76; H, 5.19; N, 16.84. GS-MS t_r = 21.4 min, *m/z* : 251 (M^+).

*5.1.4.12. 4-{4-[1-(pyridin-2-yl)-1H-pyrazol-5-yl]phenyl}morpholine (**12h**).* From 2-hydrazinopyridine dihydrochloride and **11h** (method 1). The residue was chromatographed on silica gel eluting with toluene and, then, toluene/AcOEt 1:1. The first eluate gave **12h** as a pale yellow solid, crystallized EtOH, mp 136–137 °C. Yield 28%. IR (KBr): ν 2853, 1591, 1473, 1436 cm^{-1}; ^{1}H NMR (200 MHz, (D_6) DMSO): δ 3.24–3.29 (4H, m, CH_2), 3.84–3.89 (4H, m, CH_2), 6.72 (1H, d, *J* = 1.8, H-4), 7.01 (2H, d, Ar), 7.21 (2H, d, Ar), 7.52–7.61 (1H, m, Ar), 7.72–7.78 (1H, m, Ar), 7.89 (1H, d, *J* = 1.8, H-5), 8.09–8.20 (1H, m, Ar), 8.49–8.56 (1H, m, Ar); ^{13}C NMR (50 MHz, $CDCl_3$): δ 47.3 ($2CH_2$), 65.6 ($2CH_2$), 107.1 (CH), 113.8 (2CH), 119.1 (CH), 120.4 (CH), 122.8 (CH), 128.6 (2CH), 138.6 (CH), 140.2 (C), 143.0 (CH), 147.8 (C), 150.1 (CH) 152.1 (C). Anal. Calcd. for $C_{18}H_{18}N_4O$: C, 70.57; H, 5.92; N, 18.29. Found: C, 70.35; H, 6.02; N, 18.59. GS-MS: t_r = 24.8 min, *m/z* : 306 (M^+).

*5.1.4.13. 2-[5-(2,4-dimethoxyphenyl)-1H-pyrazol-1-yl]pyridine (**12i**).* From 2-hydrazinopyridine dihydrochloride and **11i** (method 1). The residue was chromatographed on silica gel eluting with cyclohexane and, then, cyclohexane/AcOEt 7:3. The eluate gave **12i** as white solid, crystallized from cyclohexane, mp 105–107 °C. Yield 52%. IR (KBr): ν 1612, 1583, 1474, 1434 cm^{-1}; ^{1}H NMR (200 MHz, $CDCl_3$): δ 3.33 (3H, s, OCH_3), 3.87 (3H, s, OCH_3), 6.38 (1H, d, *J* = 2.4, Ar), 6.46 (1H, d, *J* = 1.6, H-4), 6.58 (1H, dd, *J* = 2.4, 8.4, Ar), 7.17–7.23 (1H, m, Ar), 7.32 (1H, d, *J* = 8.4 Hz, Ar), 7.52–7.60 (1H, m, Ar), 7.80 (1H, d, *J* = 1.6, H-3), 7.83–7.85 (1H, m, Ar), 8.36–8.40 (1H, m, Ar); ^{13}C NMR (50 MHz, $CDCl_3$): δ 53.7 (OCH_3), 54.4 (OCH_3), 97.6 (CH), 103.3 (CH), 108.1 (CH), 112.7 (C), 116.0 (CH), 120.6 (CH), 130.0 (CH), 136.7 (CH), 139.2 (C), 139.7 (CH), 146.9 (CH), 152.6 (C), 156.2 (C), 160.4 (C). Anal. calcd. for $C_{15}H_{13}N_3O_2$: C, 68.31; H, 5.37; N, 14.94; found: C, 68.42; H, 5.63; N, 14.66.

*5.1.4.14. 2-[5-(2-methoxyphenyl)-1H-pyrazol-1-yl]pyridine (**12g**); 2-[3-(2-methoxyphenyl)-1H-pyrazol-1-yl]pyridine (**13g**).* From 2-hydrazinopyridine dihydrochloride and **11g** (method 1). The residue was chromatographed on silica gel eluting with cyclohexane and, then, cyclohexane/AcOEt 7:3. The first eluate gave **13g** as a white solid, mp. Yield 10%. The second eluate gave **12g** as white solid, crystallized from cyclohexane, mp 88–90 °C. Yield 49%. Data of **12g**: IR (KBr): ν 1596, 1477, 1466, 1452, 1351 cm^{-1}; ^{1}H NMR (200 MHz, $CDCl_3$): δ 3.35 (3H, s, OCH_3), 6.51 (1H, d, *J* = 1.4, H-4), 6.80 (1H, d, *J* = 8.2, Ar), 7.02–7.09 (1H, m, Ar), 7.15–7.22 (1H, m, Ar), 7.34 (1H, d, *J* = 1.4, H-3), 7.37–7.43 (1H, m, Ar), 7.58 (1H, d, *J* = 8.2, Ar), 7.74–7.81 (2H, m, Ar), 8.26–8.33 (1H, m, Ar); ^{13}C NMR (50 MHz, $CDCl_3$): δ 54.2 (OCH_3), 109.2 (CH), 110.7 (CH), 116.4 (CH), 120.0 (CH), 120.2 (C), 120.6 (CH), 121.9 (CH), 129.6 (CH), 129.7 (CH), 138.2 (CH), 139.6 (C), 140.0 (CH), 146.9 (CH), 152.8 (C), 155.3 (C). Anal. calcd. for $C_{15}H_{13}N_3O$: C, 71.70; H, 5.21; N, 16.72; found: C, 71.68; H, 5.16; N, 16.81. Data of **13g**: IR (KBr): ν 1595, 1475, 1466, 1456, 1351, 1278 cm^{-1}; ^{1}H NMR (200 MHz, $CDCl_3$): δ 3.96 (3H, s, OCH_3), 7.02–7.31 (5H, m, Ar), 7.81–7.90 (1H, m, Ar), 8.11–8.17 (2H, m, Ar), 8.42–8.50 (1H, m, Ar), 7.43–7.52 (1H, m, Ar), 7.91–7.95 (2H, m, Ar + H-3), 8.04–8.09 (1H, m, Ar), 8.64 (1H, d, *J* = 2.4, H-5); ^{13}C NMR (50 MHz, $CDCl_3$): δ 54.5 (OCH_3), 108.5 (CH), 110.4 (CH), 111.5 (CH), 119.8 (CH), 120.0 (CH), 120.9 (C), 126.2 (CH), 127.8 (CH), 128.4 (CH), 137.5 (CH), 146.9 (CH), 149.9 (C), 150.6 (C), 156.2 (C). Anal. calcd. for $C_{15}H_{13}N_3O$: C, 71.70; H, 5.21; N, 16.72; found: C, 71.44; H, 5.61; N, 16.57.

*5.1.5. 1-(4-methoxyphenyl)-2-phenylethanone (**15b**)*

From anisole. A white solid was collected by filtration from the mixture and crystallized from cyclohexane, mp 66–67 °C. IR (KBr): ν 1676, 1601, 1574, 1335, 1260, 1172 cm^{-1}; ^{1}H NMR (200 MHz, $CDCl_3$): δ 4.02 (3H, s, OCH_3), 4.41 (2H, s, CH_2), 7.09 (2H, d, *J* = 8.8, Ar), 7.35–7.55 (5H, m, Ar), 8.17 (2H, d, *J* = 8.8, Ar). Anal. calcd. for $C_{15}H_{14}O_2$: C, 79.62; H, 6.24; found: C, 79.89; H, 5.89.

*5.1.6. 3-(dimethylamino)-1-(4-methoxyphenyl)-2-methyl-2-propen-1-one (**16a**)*

Dimethylformamide dimethylacetal (10 mmol) was added to a suspension of **15a** (10 mmol) in xylene (30 mmol) and the mixture was refluxed for 4 h. After solvent evaporation, the residue was chromatographed on silica gel eluting with cyclohexane/AcOEt 7:3 and, then, AcOEt. The first eluate gave the starting product, the

second eluate gave **16a** as a yellow oil. Yield 69%. ^{1}H NMR (200 MHz, $CDCl_3$): δ 2.28 (3H, s, CH_3), 3.16 [6H, s, $N(CH_3)_2$], 3.98 (3H, s, OCH_3), 7.02 (1H, d, J = 9.0, Ar), 7.06 (1H, s, = CH), 7.56 (2H, d, J = 9.0, Ar); Anal. calcd. for $C_{13}H_{17}NO_2$: C, 71.21; H, 7.81; N, 6.39; found: C, 71.16; H, 7.85; N, 6.33.

*5.1.7. 3-(dimethylamino)-1-(4-methoxyphenyl)-2-phenyl-2-propen-1-one (**16b**)*

Dimethylformamide dimethylacetal (10 mmol) was added to a suspension of **15b** (10 mmol) in xylene (30 mmol) and the mixture was refluxed for 2 h. After solvent evaporation, the residue was chromatographed on silica gel eluting with cyclohexane/AcOEt 7:3 and, then, AcOEt. The first eluate gave the starting product, the second eluate gave **16b** as a yellow solid, crystallized from diethyl ether, mp 92–94 °C. Yield 57%. ^{1}H NMR (200 MHz, $CDCl_3$): δ 2.90 [6H, s, $N(CH_3)_2$],3.98 (3H, s, OCH_3), 6.92 (2H, d, J = 8.8, Ar), 7.29–7.50 (5H, m, Ar + =CH), 7.55–7.61 (3H, m, Ar). Anal. calcd. for $C_{18}H_{19}NO_2$: C, 76.84; H, 6.81; N, 4.98; found: C, 76.86; H, 6.84; N, 4.95.

*5.1.8. 2-[5-(4-methoxyphenyl)-4-methyl-1H-pyrazol-1-yl]pyridine (17a); 2-[3-(4-methoxyphenyl)-4-methyl-1H-pyrazol-1-yl]pyridine (**18**)*

From 2-hydrazinopyridine dihydrochloride and **16a** (method 1) for 2 h at reflux. The residue was chromatographed on silica gel eluting with cyclohexane and, then, cyclohexane/AcOEt 8:2. The first eluate gave **18** as a yellow solid, crystallized from diethyl ether, mp 70–72 °C. Yield 8%. The second eluate gave **17a** as white solid, crystallized from cyclohexane, mp 74–75 °C. Yield 45%. Data of **17a**: IR (KBr): ν 1591, 1472, 1433, 1247 cm^{-1}; ^{1}H NMR (200 MHz, $CDCl_3$): δ 2.29 (3H, s, CH_3), 4.02 (3H, s, OCH_3), 7.07 (2H, d, J = 9.0, Ar), 7.32–7.53 (4H, m, Ar), 7.76–7.89 (2H, m, H-3 + Ar), 8. 49–8.58 (1H, m, Ar). Anal. calcd. for $C_{16}H_{15}N_3O$: C, 72.43; H, 5.70; N, 15.84; found: C, 72.14; H, 5.74; N, 15.73. Data of **18**: IR (KBr): ν 1590, 1472, 1435, 1245 cm^{-1}; ^{1}H NMR (200 MHz, $CDCl_3$): δ 2.47 (3H, s, CH_3), 4.03 (3H, s, OCH_3), 7.02–7.43 (4H, m, Ar), 7.80–7.98 (2H, m, Ar), 8.18–8.22 (1H, m, Ar), 8. 54–8.58 (1H, m, Ar + H-5). Anal. calcd. for $C_{16}H_{15}N_3O$: C, 72.43; H, 5.70; N, 15.84; found: C, 72.36; H, 5.69; N, 15.93.

*5.1.9. 2-[5-(4-methoxyphenyl)-4-phenyl-1H-pyrazol-1-yl]pyridine (**17b**)*

From 2-hydrazinopyridine dihydrochloride and **16b** (method 1) for 2 h at reflux. A white solid was collected by filtration from the mixture and crystallized from EtOH, mp 66–67 °C. Yield 73%. IR (KBr): ν 1580, 1471, 1443, 1429, 1247 cm^{-1}; ^{1}H NMR (200 MHz, $CDCl_3$): δ 3.97 (3H, s, OCH_3), 6.98 (2H, d, J = 8.4, Ar), 7.26–7.50 (9H, m, Ar), 8.80–8.89 (1H, m, Ar), 8.11(1H, s, H-3), 8.56–8.58 (1H, m, Ar). Anal. calcd. for $C_{21}H_{17}N_3O$: C, 77.04; H, 5.23; N, 12.84; found: C, 76.86; H, 5.41; N, 12.85.

*5.1.10. Synthesis of compounds **19** and **21**. General procedure:*

To a stirred suspension of sodium hydryde 60% (22.5 mmol) in dried toluene (10 mL) was slowly added a solution of 4′-methoxyacetophenone (20 mmol) and the desired ester (20 mmol) in 20 mL of dried toluene under nitrogen atmosphere. The mixture was stirred for 4 h at reflux, cooled to room temperature and quenched with a solution of HCl 10%. The organic layer was removed, and the aqueous extracted with ether. The organic layers were combined, washed with water, dried over sodium sulfate, and evaporated at reduced pressure to give the crude product.

*5.1.10.1. 1-(4-methoxyphenyl)-3-phenylpropane-1,3-dione (**19**).* From methyl benzoate. Mp 120-2 °C. Yield 68%. IR (KBr): ν 1607, 1516, 1487, 1261 cm^{-1}; ^{1}H NMR (200 MHz, $CDCl_3$) enolic form: δ 1.60 (3H, s, CH_3),3.93 (3H, s, OCH_3), 6.84 (1H, s, CH enolic form), 7.03 (2H, d, J = 8.8, Ar), 7.90 (2H, d, J = 8.8, Ar), 7.99–8.04 (5H, m, Ar). Anal. calcd. for $C_{16}H_{14}O_3$: C, 75.57; H, 5.55; found: C, 75.42; H, 5.68.

*5.1.10.2. 1-(4-methoxyphenyl)butane-1,3-dione (**21**).* From ethyl acetate. Mp 53-4 °C. Yield 51%. IR (KBr): ν 2924, 2853, 1607, 1464, 1260, 1176 cm^{-1}; ^{1}H NMR (200 MHz, $CDCl_3$) enolic form: δ 2.20 (3H, s, CH_3), 3.20 (3H, s, OCH_3), 6.15 (1H, s, CH enolic form), 6.98 (2H, d, J = 9.0, Ar), 7.54 (2H, d, J = 9.0, Ar). Anal. calcd. for $C_{11}H_{12}O_3$: C, 68.74; H, 6.29; found: C, 68.49; H, 5.41.

*5.1.11. 2-[5-(4-methoxyphenyl)-3-phenyl-1H-pyrazol-1-yl]pyridine (**20**)*

From 2-hydrazinopyridine dihydrochloride and **19** (method 1) for 2 h at reflux. A white solid was collected by filtration from the mixture and crystallized from EtOH, mp 122–123 °C. Yield 38%. IR (KBr): ν 1589, 1471, 1449, 1435, 1245 cm^{-1}; ^{1}H NMR (200 MHz, $CDCl_3$): δ 4.02 (3H, s, OCH_3), 7.00 (1H, s, H-4), 7.16 (2H, d, J = 9.0, Ar), 7.44–7.61 (7H, m, Ar), 8.03–8.12 (1H, m, Ar), 8.18–8.27 (1H, m, Ar) 8.85–8.94 (1H, m, Ar). Anal. calcd. for $C_{21}H_{17}N_3O$: C, 77.04; H, 5.23; N, 12.84; found: C, 76.98; H, 5.19; N, 12.93.

*5.1.12. 2-[5-(4-methoxyphenyl)-3-methyl-1H-pyrazol-1-yl] pyridine (**23**)*

From 2-hydrazinopyridine dihydrochloride and **21** (method 1) for 2 h at reflux. The residue was purified by chromatography on silica gel eluting with cyclohexane/AcOEt 7:3. Yield 52%. Mp 82–84 °C. IR (KBr): ν 1615, 1587, 1509, 1473, 1250 cm^{-1}; ^{1}H NMR (200 MHz, $CDCl_3$): δ 2.44 (3H, s, CH_3), 3.84 (3H, s, OCH_3), 6.31 (1H, s, H-4), 6.86 (2H, d, J = 8.8, Ar), 7.18–7.38 (4H, m, Ar), 7.67–7.77 (1H, m, Ar), 8.21–8.29 (1H, m, Ar). Anal. calcd. for $C_{16}H_{15}N_3O$: C, 72.43; H, 5.70; N, 15.84; found: C, 72.30; H, 5.69; N, 15.76.

*5.1.13. 7-(4-methoxyphenyl)-3,5,7-trioxoheptanoic acid (**22**)*

A solution of 4′-methoxyacetophenone (10 mmol) in 15 mL of dried toluene was added to a stirred suspension of sodium amide (20 mmol) in dried toluene (40 mL). The mixture was stirred for 20 min at 50 °C, then AcOEt (11 mmol) was added slowly. The resulting mixture was heated at reflux overnight, cooled to room temperature, and quenched with water (20 mL). The organic layer was removed, and the aqueous acidified with HCl 37%, followed by extraction with ether. The organic layers were combined, washed with water (20 mL), dried over sodium sulfate, and evaporated at reduced pressure to give the crude product as an oil. The residue was chromatographed on silica gel eluting with toluene and, then, toluene/AcOEt 1:1. The title compound was obtained as a white solid from $CHCl_3$, mp. 143–145 °C. Yield 29%. IR (KBr): ν 3364, 1682, 1658, 1605 cm^{-1}; ^{1}H NMR (200 MHz, $CDCl_3$): δ 3.50 (4H, s, CH_2), 4.00(3H, s, OCH_3), 7.22 (2H, d, J = 8.8, Ar), 7.87 (2H, d, J = 8.8, Ar), 13.02 (1H, s, COOH). Anal. calcd. for $C_{12}H_{12}O_5$: C, 61.01; H, 5.12; found: C, 61.28; H.

*5.1.14. 2-[5-(4-methoxyphenyl)-1-(pyridin-2-yl)-1H-pyrazol-3-yl] acetic acid (**24**)*

From 2-hydrazinopyridine dihydrochloride and **22** (method 1) for 2 h at reflux. The residue was purified by chromatography on silica gel eluting with toluene and, then, AcOEt. The second eluate gave **24** as white solid, crystallized from cyclohexane, mp 169–172 °C. Yield 18%. IR (KBr): ν 3000 (br), 1601, 1511, 1483, 1438, 1253 cm^{-1}; ^{1}H NMR (200 MHz, $CDCl_3$): δ 2.39 (2H, s, CH_2), 3.91 (3H, s, OCH_3), 6.84–6.91(2H, m, Ar + H-4), 6.95 (2H, d, J = 8.8, Ar), 7.45–7.51 (1H, m, Ar), 7.58 (2H, d, J = 8.8, Ar). Anal. calcd. for $C_{17}H_{15}N_3O_3$: C, 66.01; H, 4.89; N, 13.58; found: C, 66.06; H, 5.01; N, 12.95.

5.2. Biology

5.2.1. MTT assay

Human cell lines A2780 (ovary, adenocarcinoma) and A549 (lung, carcinoma), and murine P388 (leukemia) cells were plated (P388: 900 cells/well; A549: 1600 cells/well; A2780: 2000 cells/well) into flat-bottomed (for adherent cells) and U-bottomed (for non-adherent cells) 96-well microtiter plates, treated for 72 h with 5 concentrations of our pyrazole derivatives (1:10 fold concentrations) and prepared as described elsewhere [47,48].

5.2.2. Morphological determination of apoptotic cells by 4′-6-diamidino-2-phenylindole (DAPI)

Apoptosis was evaluated in all cell lines for the four pyrazole derivatives that demonstrated to be more active by the MTT assay. Cells (from 5×10^3 to 11×10^3) were plated in 1 mL of culture medium into 24-well plates and treated with the IC_{50} and IC_{90} equitoxic concentrations, as determined by the MTT assay. Floating and adherent cells were harvested after 3 days culture, washed with cold phosphate buffered saline (PBS) and resuspended in 100 μL of 70% ethanol in PBS. Samples were maintained at 4 °C until microscopic examination. For the morphological analysis of nuclei, 5 μL of a solution of 10 mg/mL DAPI in water were added and the percentage of apoptotic segmented nuclei/cells stained with the fluorescent dye evaluated ($n = 3–7$).

5.2.3. Analysis of the cell cycle

P388 cells were also analyzed for the effect of active compounds on cell cycle phases. To this end cells (5×10^3 in 3–4 mL of complete medium) were treated for 24, 48 and 72 h with the IC_{30} and IC_{75} of our molecules, harvested, washed twice with cold PBS, and fixed in 70% ethyl alcohol overnight at −20 °C. The day after they were centrifuged, washed with cold PBS and incubated at room temperature for 20 min with propidium iodide (PI) staining solution (50 μg/mL PI, 0.05% Triton X-100, 0.2 mg/mL RNase A in PBS). Cells were finally analyzed by flow cytometric analysis of DNA content using FACSort flow cytometer (BD Biosciences, Mountain. View, CA). Doublets, cell clumps, and debris were excluded by plotting PI fluorescence pulse-width versus pulse-area measurements using CellQuest software (BD Biosciences). Cell cycle analysis on the gated PI distribution was performed using Modfit software.

5.2.4. Western blot analysis of p53 and $p21^{waf1}$

In a single experiment human A2780 and A549 cells were treated with 0.1, 10, and 100 μM **12d**. After 24, 48 and 72 h culture cells were harvested, washed twice with cold PBS and lysed for 30 min at 4 °C with a buffer containing 1% Triton X-100, 0.15 M NaCl, 10 mM Tris (pH 7.4), 0.1 mg/mL phenylmethylsulphonyl fluoride and 50 μg/mL aprotinin. The protein concentration was determined by the Bradford method (Sigma Chemical Co., St. Louis, MO, USA). Fifty mg of protein were separated on a 12% polyacrylamide gel (SDS-PAGE) and then transferred onto a nitrocellulose membrane (Hybond C-Extra, Amersham Italia Srl, Milan, Italy). The protein loading was checked by Ponceau S staining. Nonspecific binding was blocked overnight at 4 °C with 2% bovine albumin (Sigma) in Tris-buffered saline-Tween 20 [0.15 M NaCl, 10 mM Tris (pH 8.0), 0.05% Tween 20]. Blots were probed with anti-p53 DO-1 (1:2,000, Santa Cruz, CA, USA), anti-$p21^{waf1}$ 1:1000 (Exbio, Praha, Czech Republic) and anti-α-tubulin (1:2,000, Santa Cruz) monoclonal antibodies. The membranes were then incubated with horseradish peroxidase-conjugated anti-mouse IgG and bands visualized by chemiluminescent detection (ECL™ Western blotting analysis system, Amersham Italia Srl) following the supplier's recommended procedures. Prestained molecular weight markers (New England Biolabs, Beverly, MA, USA) were used as reference. The expression signal obtained by an anti-β-actin monoclonal antibody (TU-02,1:5,000, Santa Cruz, CA, USA) was used for the densitometric normalization.

5.2.5. Microtubule immunofluorescence

Ten to five A549 cells were cultured in chamber slides and 24 h later treated with 1, 10 and 100 μM of selected active substances and with 100 nM taxol as positive control. After 24-h incubation A549 cells were washed with cold PBS and fixed at room temperature for 5 min with 3.7% paraformaldehyde in PBS plus 2% sucrose (PBS-S). Once washed again 3 times with cold PBS-S on ice, they were incubated with methanol for other 5 min at −20 °C. Further 3 additional washes with cold PBS-S ended the fixation procedure. Thirty min incubation with cold 20% goat serum in PBS (GS-PBS) on ice was used to saturate non-specific immunoglobulin binding sites. The monoclonal anti-α-tubulin (T5168, Sigma) diluted 2000 times in GS-PBS was added for 2 h on ice, then cells were washed 3 times with cold PBS-S on ice. The Alexa 594 goat anti-mouse IgG1 (2.5 μg/mL in GS-PBS) was used to reveal the anti-α-tubulin antibody after incubation on ice for 30 min. The samples were finally washed 3 times with cold PBS-S on ice and the slide mounted with a coverslip using GelMount (Biomeda Inc., CA). Images were acquired with an Axiovert 200M microscope (Carl Zeiss Micro-Imaging GmbH, Goettingen, Germany).

5.2.6. Tubulin polymerization assay

The effect of tested compounds on in vitro assembly of tubulin microtubules was evaluated using a fluorescence-based microtubule polymerization assay kit (Cytoskeleton, Denver, USA) [49,50], following the recommended protocol. Briefly, porcine brain tubulin was dissolved in 80 mM piperazine-N,N′-bis[2-ethanesulfonic acid] sequisodium salt, 2 mM magnesium chloride, 0.5 mM ethylene glycol-bis(β-amino-ethyl ether) N,N,N′,N′-tetra-acetic-acid, 60% v/v glycerol, pH 6.9. The assay was carried out in a half area 96-well plate (Corning Costar), and the reaction was initiated by the addition of tubulin. The plate was incubated at 37 °C on a fluorescence microplate reader (Mithras LB 940, Berthold Technologies), and microtubule assembly was monitored by measuring fluorescence (λex, 355 nm; λem, 460 nm) by the minute for 60 min. A tubulin polymerization assay was performed in the presence of 10, 2, 1 and 0.5 μM concentrations of **12a**, **12a1**, **12d1** and **12d** compounds and results compared with untreated controls containing fetal calf serum plus 4% DMSO. Positive controls were treated with 3 μM taxol and 1.6 μM vincristine.

5.2.7. Preparation of ligands and receptor molecules for docking

A molecular structure of the selected compound was built and energy minimized with the programs Insight II and Discover3 (Biosym/MSI, San Diego, CA, USA). To analyze the receptor–ligand complexes, we used the atomic coordinates of the alpha-beta tubulin dimer [38]. The receptor and the ligands were prepared for docking using ADT, the AutoDock tool graphical interface [51]. For each receptor structure polar hydrogens were added, Kollman charges were assigned and atomic solvatation parameters were added. Polar hydrogen charges of the Gasteiger-type were assigned and the non-polar hydrogens were merged with the carbons, the internal degrees of freedom and torsions were set for all the designed small molecules. The resulting atomic models were then submitted to different cycles of molecular dynamics followed by energy minimization using the programs Insight II and Discover3. The resulting model was used as target for molecular docking simulations using the program AutoDock 3.05 [52].

5.2.8. Docking simulation

To better address our search, we performed three different simulations using, as targets, the alpha monomer, the beta

monomer and the alpha-beta dimer respectively. For each simulation, in a first phase, **12d** was docked into the active site using the program AutoDock 3.05 with the macromolecule considered as a rigid body and the ligand being flexible. The searching grid was extended over the whole receptor protein. Affinity maps for all the atom types present, as well as an electrostatic map, were computed with a grid spacing of 0.375 Å. The search was carried out with the Lamarckian Genetic Algorithm: populations of 256 individuals with a mutation rate of 0.02 were evolved for 100 generations.

Evaluation of the results was performed by sorting the different complexes with respect to the predicted binding energy. A cluster analysis based on root mean square deviation values, with reference to the starting geometry, was subsequently performed and the lowest energy conformation of the more populated cluster was considered as the most promising bioactive candidate.

In a second phase, we validated the correct positioning of the ligands within the active site cleft by using a second docking program, GOLD (CCDC, Cambridge, UK) which also allowed us to calculate a fitness function (Goldscore) for the complex.

Acknowledgment

Financial support from Italian MIUR is gratefully acknowledged. The authors thank Prof. Olga Bruno for the helpful discussions and suggestions.

References

[1] J. Elguero, P. Goya, N. Jagerovic, A.M.S. Silva, in: O.A. Attanasi, D. Spinelli (Eds.), Targets in Heterocyclic Systems, 6th ed. Società Chimica Italiana, Roma, 2002, pp. 52–98.
[2] G. Szabo, J. Fischer, A. Kis-Varga, K. Gyires, J. Med. Chem. 51 (2008) 142–147.
[3] A. Tanitame, Y. Oyamada, K. Ofuji, H. Terauchi, M. Kawasaki, M. Wachi, J. Yamagishi, Bioorg. Med. Chem. Lett. 15 (2005) 4299–4303.
[4] A. Tanitame, Y. Oyamada, K. Ofuji, M. Fujimoto, K. Suzuki, T. Ueda, H. Terauchi, M. Kawasaki, K. Nagai, M. Wachi, J. Yamagishi, Bioorg. Med. Chem. 12 (2004) 5515–5524.
[5] N. Cho, M. Kamaura, T. Yogo, H. Imoto, PCT Int. Appl. (2009) WO 2009139340.
[6] K. Dugi, M. Mark, F. Himmelsbach, PCT Int. Appl. (2009) WO 2009022009.
[7] Y. Momose, T. Maekawa, H. Odaka, H. Kimura, PCT Int. Appl. (2001) WO 2001038325.
[8] S.M. Rida, M.N.S. Saudi, A.M. Youssef, M.A. Halim, Lett. Org. Chem. 6 (2009) 282–288.
[9] J. Regan, S. Breitfelder, P. Cirillo, T. Gilmore, A.G. Graham, E. Hickey, B. Klaus, J. Madwed, M. Moriak, N. Moss, C. Pargellis, S. Pav, A. Proto, A. Swinamer, L. Tong, C. Torcellini, J. Med. Chem. 45 (2002) 2994–3008.
[10] M.G. Brasca, C. Albanese, R. Amici, D. Ballinari, L. Corti, V. Croci, D. Fancelli, F. Fiorentini, M. Nesi, P. Orsini, F. Orzi, W. Pastori, E. Perrone, E. Pesenti, P. Pevarello, F. Riccardi-Sirtori, F. Roletto, P. Roussel, M. Varasi, A. Vulpetti, C. Mercurio, Chem. Med. Chem. 2 (2007) 841–852.
[11] P. Pevarello, D. Fancelli, A. Vulpetti, R. Amici, M. Villa, V. Pittalà, P. Vianello, A. Cameron, M. Ciomei, C. Mercurio, J.R. Bischoff, F. Roletto, M. Varasi, M.G. Brasca, Bioorg. Med. Chem. Lett. 16 (2006) 1084–1090.
[12] A.H. Abadi, A. Abdel Haleem Eissa Hassan, G.S. Hassan, Chem. Pharm. Bul 51 (2003) 838–844.
[13] M.R. Michaelides, PCT Int. Appl. (2010) WO 2010065825.
[14] S. Ludwig, O. Planz, Hans-H. Sedlacek, S. Pleschka, PCT Int. Appl. (2004) WO 2004085682.
[15] E.M. Perchellet, M.M. Ward, Alexios-L. Skaltsounis, I.K. Kostakis, N. Pouli, P. Marakos, J.H. Perchellet, Anticancer Res. 26 (2006) 2791–2804.
[16] B. Insuasty, A. Tigreros, F. Orozco, J. Quiroga, R. Abonia, M. Nogueras, A. Sanchez, J. Cobo, Bioorg. Med. Chem. 18 (2010) 4965–4974.
[17] M. Labbozzetta, R. Baruchello, P. Marchetti, M.C. Gueli, P. Poma, M. Notarbartolo, D. Simoni, N. D'Alessandro, Chem.-Biol. Interact 181 (2009) 29–36.
[18] P. Pevarello, M.G. Brasca, R. Amici, P. Orsini, G. Traquandi, L. Corti, C. Piutti, P. Sansonna, M. Villa, B.S. Pierce, M. Pulici, P. Giordano, K. Martina, E.L. Fritzen, R.A. Nugent, E. Casale, A. Cameron, M. Ciomei, F. Roletto, A. Isacchi, G.P. Fogliatto, E. Pesenti, W. Pastori, A. Marsiglio, K.L. Leach, P.M. Clare, F. Fiorentini, M. Varasi, A. Vulpetti, M.A. Warpehoski, J. Med. Chem. 47 (2004) 3367–3380.
[19] M. Anzaldi, E. Sottofattori, R. Rizzetto, B. Granello Di Casaleto, A. Balbi, Eur. J. Med. Chem. 34 (1999) 837–842.
[20] A. Balbi, M. Anzaldi, M. Mazzei, M. Miele, M. Bertolotto, L. Ottonello, F. Dallegri, Bioorg. Med. Chem. 14 (2006) 5152–5160.
[21] M. Anzaldi, C. Macciò, M. Mazzei, M. Bertolotto, L. Ottonello, F. Dallegri, A. Balbi, Chem. Biodivers 6 (2009) 1674–1687.
[22] S. Al-Mousawi, M.M. Abdel-Khalik, S. El-Sherbiny, E. John, M.H. Elnagdi, J. Heterocycl. Chem. 38 (2001) 949–953.
[23] Y. Lin, S.A. Lang Jr., J. Org. Chem. 45 (1980) 4857–4860.
[24] T. Ghosh, S. Saha, C. Bandyopadhyay, Synthesis 11 (2005) 1845–1849.
[25] W. Loewe, A. Kennemann, Arch. Pharm. 318 (1985) 239–243.
[26] J.P. Dusza, A.S. Tomcufcik, J.D. Albright, Eur. Pat. Appl. (1985) EP 129847.
[27] C.K. Ghosh, S. Khan, Synthesis 9 (1981) 719–721.
[28] S.S. Tseng, J.W. Epstein, H.J. Brabander, G. Francisco, J. Heterocycl. Chem. 24 (1987) 837–843.
[29] S.S. Tseng, J.P. Dusza, J.W. Epstein, U. S. P. (1989) US 4888345.
[30] Y.D. Wang, A. Gopalsamy, D.W. Powell, H. Tsou, N. Zhang, U. S. Pat. Appl. (2006) 20060063785.
[31] A.M.S. Silva, L.M.P.M. Almeida, J.A.S. Cavaleiro, C. Foces-Foces, A.L. Llamas-Saiz, C. Fontenas, N. Jagerovic, J. Elguero, Tetrahedron 53 (1997) 11645–11658.
[32] G.A. Reynolds, J.A. Van Allan, A.K. Seidel, J. Heterocycl. Chem. 16 (1979) 369–370.
[33] (a) J.C. Jung Lee, J.H. Lee, S. Oh, J.G. Lee, O.S. Park, Bioorg. Med. Chem. Lett. 14 (2004) 5527–5531;
(b) S.S. Jenkins, J. Am. Chem. Soc. 54 (1932) 1155–1163.
[34] E. Hasegawa, K. Ishiyama, T. Horaguchi, T. Shimizu, J. Org. Chem. 56 (1991) 1631–1635.
[35] A. Horeau, J. Jacques, Bull. Soc. Chim. Fr. (1948) 53–59.
[36] M.A. Jordan, D. Thrower, L. Wilson, J. Cell Sci. 102 (1992) 401–416.
[37] E.L.K. Goh, T.J. Pircher, P.E. Lobie, Endocrinology 139 (1998) 4364–4372.
[38] B. Gigant, C. Wang, R.B. Ravelli, F. Roussi, M.O. Steinmetz, P.A. Curmi, A. Sobel, M. Knossow, Nature 435 (2005) 519–522.
[39] H. Ohki, K. Hirotani, H. Naito, S. Ohsuki, M. Minami, A. Ejima, Y. Koisoc, Y. Hashimoto, Bioorg. Med. Chem. Lett. 12 (2002) 3191–3193.
[40] M. Iwahana, Y. Ochi, A. Ejima, Anticancer Res. 20 (2000) 785–792.
[41] C. Wasylyk, H. Zheng, C. Castell, L. Debussche, M.C. Multon, B. Wasylyk, Cancer Res. 68 (2008) 1275–1283.
[42] S. Bergemann, R. Brecht, F. Büttner, D. Guénard, R. Gust, G. Seitz, M.T. Stubbs, S. Thoret, Bioorg. Med. Chem. 11 (2003) 1269–1281.
[43] V. Agnese, V. Bazan, F.P. Fiorentino, D. Fanale, G. Badalamenti, G. Colucci, V. Adamo, D. Santini, A. Russo, Ann. Oncol. 18 (2007) 47–52 Supp vi.
[44] J.R. Pollard, M. Mortimore, J. Med. Chem. 52 (2009) 2629–2651.
[45] D.O. Wise, R. Krahe, B.R. Oakley, Genomics 67 (2000) 164–170.
[46] T. Nayak, H. Edgerton-Morgan, T. Horio, Y. Xiong, C.P. De Souza, S.A. Osmani, B.R. Oakley, J. Cell. Biol. 190 (2010) 317–330.
[47] S. Cafaggi, E. Russo, R. Stefani, R. Leardi, G. Caviglioli, B. Parodi, G. Bignardi, D. De Totero, C. Aiello, M. Viale, J. Control. Release 121 (2007) 110–123.
[48] R.F. Hussain, A.M.E. Nouri, R.T.D. Oliver, J. Immunol. Methods 160 (1993) 89–96.
[49] D. Bonne, C. Heusele, C. Simon, D. Pantaloni, J. Biol. Chem. 260 (1985) 2819–2825.
[50] D.M. Barron, S.K. Chatterjee, R. Ravindra, R. Roof, E. Baloglu, G.I. David, D.G.I. Kingston, S. Bane, Anal. Biochem. 315 (2003) 49–56.
[51] M.F. Sanner, B.S. Duncan, C.J. Carrillo, A.J. Olson, Symp. Biocomput 4 (1999) 401–412.
[52] D.S. Goodsell, G.M. Morris, A.J. Olson, J. Mol. Recognit 9 (1996) 1–5.